

Non-perturbative effects of vacuum energy on the recent expansion of the universe

Leonard Parker* and Alpan Raval†

Department of Physics, University of Wisconsin-Milwaukee, P.O. Box 413, Milwaukee, WI 53201.

We show that the vacuum energy of a free quantized field of very low mass can significantly alter the recent expansion of the universe. The type of particle we consider is of spin-0, but a higher spin field, such as a graviton of ultralight mass, may well affect the expansion in the same way. The effective action of the theory is obtained from a non-perturbative sum of scalar curvature terms in the propagator. We renormalize this effective action and express it in terms of observable gravitational coupling constants. We numerically investigate the semiclassical Einstein equations derived from it. As a result of non-perturbative quantum effects, the scalar curvature of the matter-dominated universe stops decreasing and approaches a constant value. The universe in our model evolves from an open matter-dominated epoch to a mildly inflating de Sitter expansion. The Hubble constant during the present de Sitter epoch, as well as the time at which the transition occurs from matter-dominated to de Sitter expansion, are determined by the mass of the field and by the present matter density. The model provides a theoretical explanation of the observed recent acceleration of the universe, and gives a good fit to data from high-redshift Type Ia supernovae, with a mass of about 10^{-33} eV, and a current ratio of matter density to critical density, $\Omega_0 < 0.4$. The age of the universe then follows with no further free parameters in the theory, and turns out to be greater than 13 Gyr. The model is spatially open and consistent with the possibility of inflation in the very early universe. Furthermore, our model arises from the standard renormalizable theory of a free quantum field in curved spacetime, and does not require a cosmological constant or the associated fine-tuning. PACS numbers: 98.80.Cq, 04.62.+v, 98.80.-k, 98.80.Es

WISC-MILW-99-TH-6

April 28, 1999.

arXiv:gr-qc/9905031v2 11 Jun 1999

*Electronic address: leonard@uwm.edu

†Electronic address: raval@uwm.edu

I. INTRODUCTION

There appear to be deep connections between phenomena at the microscopic quantum level and those at the macroscopic level described by general relativity. These connections were first elucidated by studies of quantum field theory in the classical curved spacetime of general relativity, particularly those involving particle creation by strong gravitational fields, such as exist in the early universe and near black holes [1,2]. The framework of quantum field theory in the classical curved spacetime of general relativity appears to be quite robust, and is the one we employ in our present study. We are particularly concerned with certain non-perturbative gravitational contributions to the vacuum energy of quantized fields [3].

We show that these contributions may account for the recent observations [5,6] of type-Ia supernovae (SNe-Ia) that seem to imply that there is an acceleration of the recent expansion of the universe. In our model, the key new ingredient needed to account for the observations is the existence of a particle having a very small mass of about 10^{-33} eV. This could be a scalar particle or one of higher spin, such as a graviton. It is well-known that in a Robertson-Walker universe, the linearized Einstein equations obeyed by the graviton field take the same form (for each polarization in the Lifshitz gauge) as the equation of a minimally coupled massless scalar field [7]. Inclusion of a mass of about 10^{-33} eV in these equations would give effects similar to the ones studied here, and would evidently not conflict with other observations. We consider a scalar field for simplicity.

The effects we investigate stem from the discovery [3,8] that a covariant infinite series of terms in the propagators of quantum fields in curved spacetime can be summed in closed form, to all orders in the curvature. The summed infinite series of terms are *all* those that involve at least one factor of the scalar curvature, R , (together with any number of factors of the Riemann tensor and its covariant derivatives) in the Schwinger-DeWitt proper-time series for the propagator. We will refer to this partially-summed form of the propagator as the R -summed form of the propagator. Although only the first several terms in the proper-time series have been calculated (because of their complexity), the R -summed form can be derived by means of mathematical induction [8]. A further reason to expect the R -summed form of the propagator to contain information of physical significance, is that the leading term in the R -summed form of the propagator follows directly from the Feynman path-integral expression for the propagator by means of a Gaussian integration about the dominant path [9]. Our results flow from the effective action that is obtained from the R -summed form of the propagator.

We leave for a later paper, the contribution of these non-perturbative gravitational effects to early inflation at the grand-unified scale and associated particle creation. In this paper, we focus on possible consequences of these non-perturbative terms in the effective action that may be observed today. As noted earlier, we find that these non-perturbative effects in the presence of an ultralight particle having a mass of about 10^{-33} eV, give a good fit to the observed SNe-Ia data points. The effective action of our model has a single free parameter determined by the mass of the particle and its curvature coupling constant. In addition, there are two more parameters which characterize the solutions to the effective gravitational field equations. These can be taken to be the present Hubble constant and the present matter density. The Hubble constant is determined by low redshift measurements as usual. The mass of the particle, and the present matter density are given by a fit to the SNe-Ia data. The age of the universe, and the cosmic time, or red-shift, at which the non-perturbative contributions of the ultralight particle first become significant, follow from these parameters.

Our model involves a renormalizable free field theory in curved spacetime, and apart from the supposed existence of an ultralight mass, is based on previously discovered non-perturbative terms. Furthermore, it requires no cosmological constant in the usual sense of the term; and no fine-tuning of the value of the current cosmic time is necessary to explain the current observed value of the matter density.

The outline of this paper is as follows. In Sec. II, we calculate, by zeta-function regularization, the renormalized effective action that follows from the R -summed propagator. This confirms the result found with dimensional regularization by Parker and Toms [3], and generalizes it to include the case when there is an imaginary part of the effective action. Variation of this effective action gives the Einstein gravitational field equations, including vacuum contributions of quantized fields. In addition, an imaginary part of the effective action implies a rate of particle creation in the same way as it does in quantum electrodynamics [10]. The effective action has infrared-type divergences which are treated separately in Appendix A.

The effective action at low curvatures gives rise to induced gravitational coupling constants, as is well-known. These constants depend on a renormalization scale parameter. In Section III, we consider the dependence of the induced gravitational constants on the renormalization scale, and identify the renormalized constants with their known values at low curvature. This identification is used to fix all the coupling constants in the effective action, in terms of their low curvature values, except the field mass m and its curvature coupling ξ . In this context, the conclusions of Ref. [3] are explored in greater detail and generalized here. Variations of various terms in the effective action are listed in Appendix B.

In Section IV, we clarify the meaning of exact and perturbative solutions to the semiclassical Einstein equations. In particular, we emphasize that a perturbative treatment in \hbar must be done in such a way that only genuine quantum corrections are treated in a perturbative manner, while factors of \hbar which occur in the “classical” Klein-Gordon action are not treated perturbatively.

In Section V, we display a set of constant curvature (de Sitter) solutions¹, which exist even in the absence of an explicit cosmological constant term in the effective action. We show that, for $\xi - 1/6 > 0$, such solutions typically have Planckian curvatures and are therefore not of much physical interest. On the other hand, for $\xi - 1/6 < 0$, we show that there exist de Sitter solutions with scalar curvature approximately equal to $m^2/(1/6 - \xi)$, and that such solutions exist for a wide range of values of m and ξ . As argued in later sections, these solutions could play a vital role at the present time, if there exists an ultralight particle with $\xi - 1/6 < 0$. In Section VI, we carry out perturbative calculations of the scalar curvature about a classical Robertson-Walker universe, containing classical matter and radiation. We find that quantum corrections to the classical scalar curvature of the universe can become significant at an epoch determined by the mass scale $\overline{m} = m/\sqrt{1/6 - \xi}$, for $\xi - 1/6 < 0$. Furthermore, we find that the quantum corrections tend to drive the scalar curvature to a constant value. These considerations lead to a scenario, presented in Section VII, in which quantum corrections to a matter-dominated universe cause a transition to a de Sitter solution of the type discussed in Section V. The various cosmological parameters in such a model universe are expressed in terms of three basic parameters to be determined by observation: the mass scale \overline{m} , the present ratio of matter density to critical density Ω_0 , and the present Hubble constant H_0 .

In Section VIII, we develop this scenario further, using it to obtain magnitude-redshift curves, and comparing these curves to recent data from high-redshift Type 1a supernovae [6]. The mass scale \overline{m} is determined to be roughly equal to 10^{-33} eV, while Ω_0 is found to be less than 0.4. In Section IX, we derive from these parameters the age of the universe in our model, which is found to be greater than about 13 Gyr. Finally, in Section IX, we conclude with a discussion of our results and comment on future work.

The main results of this paper are summarized in Eqs. (38) and (43) (the effective action of the theory in terms of measurable gravitational coupling constants), Eq. (53) (the relationship between scalar curvature and mass during the late de Sitter phase), Eq. (86) (the scale factor in our model), Eq. (109) and the equations prior to it in Section VIII (the luminosity-distance-redshift relation), the discussion of the age of the universe in Section IX, and Figs. 3 and 4.

Throughout this paper, we use the metric signature convention $(-+++)$, and the convention for the Riemann curvature tensor $R_{\mu\nu\rho}{}^\sigma = \Gamma^\sigma_{\mu\rho,\nu} - \Gamma^\sigma_{\nu\rho,\mu} + \Gamma^\alpha_{\mu\rho}\Gamma^\sigma_{\alpha\nu} - \Gamma^\alpha_{\nu\rho}\Gamma^\sigma_{\alpha\mu}$.

II. QUANTUM CORRECTIONS TO EFFECTIVE ACTION

Here we derive the regularized effective action based on the propagator for a scalar field in curved space.

Parker and Toms [3] define the effective action via dimensional regularization of the Feynman Green function and by integrating the Green function with respect to the square of the mass. Here we will define it by zeta-function regularization.

To this end, consider a D -dimensional scalar field theory in curved spacetime, with classical action

$$S = -\frac{1}{2} \int d^D x \phi(x) H(x) \phi(x), \quad (1)$$

where $H(x) = -g_{\mu\nu}(x) \nabla_x^\mu \nabla_x^\nu + m^2 + \xi R(x)$, and we have ignored boundary contributions. The one-loop effective action, W^1 , is defined by the functional integral

$$e^{iW^1} \equiv Z = \int D\phi e^{iS}, \quad (2)$$

and is related to the transition amplitude for evolution from the “in” vacuum state at early times to the “out” vacuum state at late times [10]:

$$e^{iW^1} = \langle 0_{\text{out}} | 0_{\text{in}} \rangle. \quad (3)$$

¹de Sitter solutions to the effective gravitational field equations have been found by other authors in gravity theories with higher derivative terms [4,16]. These solutions are valid at high curvatures. In this paper, we also find low-curvature de Sitter solutions which could play an important role in the late evolution of the universe.

For free fields, as considered here, the one-loop effective action, W^1 , gives the *full* quantum contributions of the matter field to the effective action. By formally performing the functional integral in Eq. (2), we get (see, for example [13])

$$W^1 = \frac{i}{2} \ln \det(H/\mu^2), \quad (4)$$

where we have introduced an arbitrary real quantity μ with the dimensions of mass in order to render Z dimensionless.

In terms of the zeta function, formally defined as

$$\zeta(\nu) = \text{Tr } H^{-\nu}, \quad (5)$$

the one-loop effective action can be expressed in the form

$$W^1 = -\frac{i}{2} [\zeta'(0) + \ln(\mu^2)\zeta(0)]. \quad (6)$$

The proper-time heat kernel, K , is defined to satisfy the equation

$$\left(i \frac{\partial}{\partial s} - H(x) \right) K(x, x', is) = 0, \quad (7)$$

with initial condition

$$K(x, x', 0) = (-g)^{-\frac{1}{2}} \delta^{(D)}(x - x'). \quad (8)$$

Because Eq. (7) is a Schrodinger-like equation, the heat kernel may be formally represented as

$$K(x, x', is) = \langle x | e^{-isH} | x' \rangle, \quad (9)$$

with the inner product $\langle x | x' \rangle$ defined by Eq. (8).

The heat kernel gives a representation for the Feynman Green's function of the theory:

$$G(x, x') \equiv \langle x | H^{-1} | x' \rangle = \int_0^\infty ids \langle x | e^{-is(H-i\epsilon)} | x' \rangle, \quad (10)$$

where we have added a small imaginary part to H for reasons of convergence.

Also, using the Mellin transform to express the zeta function in terms of the heat kernel, one obtains

$$\zeta(\nu) = \Gamma(\nu)^{-1} \int d^D x \sqrt{-g} \int_0^\infty ids (is)^{\nu-1} \langle x | e^{-is(H-i\epsilon)} | x \rangle. \quad (11)$$

We now introduce the R -summed form of the heat kernel [3,8]

$$\langle x | e^{-is(H-i\epsilon)} | x' \rangle = i(4\pi is)^{-D/2} \Delta^{\frac{1}{2}}(x, x') e^{i\frac{\sigma}{2s} - is(M^2 - i\epsilon)} \bar{F}(x, x'; is), \quad (12)$$

where $\Delta(x, x')$ is the Van Vleck-Morette determinant and $\sigma(x, x')$ is one-half the square of the geodesic distance between x and x' . The quantity M^2 is, in general, a function of x and x' with the property that it reduces in the coincidence limit to

$$M^2(x, x) = m^2 + (\xi - 1/6)R(x) \equiv m^2 + \bar{\xi}R(x), \quad (13)$$

where $\bar{\xi} \equiv \xi - 1/6$. The form (12) of the heat kernel sums all terms explicitly involving at least one factor of the scalar curvature R , in the coincidence limit $x' \rightarrow x$. Away from the coincidence limit, M^2 can be taken to be the linear combination [8]

$$M^2(x, x') = m^2 + \bar{\xi}(aR(x) + (1-a)R(x')) \quad (14)$$

with an arbitrary choice of a , and the function \bar{F} will correspondingly depend on the value of a . \bar{F} may be expanded in an asymptotic series in powers of s , namely,

$$\bar{F}(x, x'; is) \approx \sum_{j=0}^{\infty} (is)^j \bar{f}_j(x, x'), \quad (15)$$

In the coincidence limit $x' \rightarrow x$, \bar{F} does not depend on a . We then have $\bar{f}_0(x, x) = 1$, $\bar{f}_1(x, x) = 0$, and

$$\bar{f}_2(x, x) = \frac{1}{6} \left(\frac{1}{5} - \xi \right) \square R + \frac{1}{180} (R_{\alpha\beta\gamma\delta} R^{\alpha\beta\gamma\delta} - R_{\alpha\beta} R^{\alpha\beta}). \quad (16)$$

The \bar{f}_j for all j contain no factor of R (with no derivatives acting on it).

Thus Eq. (11) becomes

$$\zeta(\nu) = i(4\pi)^{-D/2} \Gamma(\nu)^{-1} \int d^D x \sqrt{-g} \int_0^\infty ds (is)^{\nu-1-D/2} e^{-is(M^2-i\epsilon)} \bar{F}(x, x; is). \quad (17)$$

The integral over s in the above expression is divergent at $\nu = 0$ because of the singular behavior of the integrand as s approaches zero. This divergence actually exists for all $\text{Re } \nu \leq D/2$. [We will assume throughout this paper that D is even]. We therefore regulate the zeta function for these values of ν by defining the zeta function for $\text{Re } \nu \leq D/2$ as the analytic continuation of the zeta function for $\text{Re } \nu > D/2$. To this end, we perform $D/2 + 1$ integrations by parts before analytically continuing, to get

$$\zeta(\nu) = -i(-4\pi)^{-D/2} \frac{\Gamma(\nu)^{-1}}{(\nu - D/2)(\nu - D/2 + 1) \cdots \nu} \int d^D x \sqrt{-g} \int_0^\infty ds (is)^\nu \times \frac{\partial^{D/2+1}}{\partial (is)^{D/2+1}} \left(e^{-is(M^2-i\epsilon)} \bar{F}(x, x; is) \right), \quad (18)$$

which is regular in a neighborhood of $\nu = 0^2$. This definition of the ζ function therefore leads to a regularised one-loop effective action. From Eqs. (6) and (18), we get

$$W^1 = \{2(4\pi)^{D/2} (D/2)!\}^{-1} \int d^D x \sqrt{-g} \left\{ \left(\gamma + \ln(\mu^2) + \frac{1}{D/2} + \frac{1}{D/2-1} + \cdots + 1 \right) \times \frac{\partial^{D/2}}{\partial (is)^{D/2}} \left(e^{-is(M^2-i\epsilon)} \bar{F}(x, x; is) \right)_{s=0} - \int_0^\infty ds \ln(is) \frac{\partial^{D/2+1}}{\partial (is)^{D/2+1}} \left(e^{-is(M^2-i\epsilon)} \bar{F}(x, x; is) \right) \right\}, \quad (19)$$

where $\gamma = \text{Euler's constant} = \frac{d}{d\nu} [\Gamma(\nu + 1)]_{\nu=0}$.

Fixing the renormalization scale μ is equivalent to fixing the (constant) phase of the out-vacuum relative to the in-vacuum in flat space, which can be chosen arbitrarily. We will find it convenient to define a rescaled version of μ by $\ln(\tilde{\mu}^2) = \ln(\mu^2) + \frac{1}{D/2} + \frac{1}{D/2-1} + \cdots + 1$. Then the one-loop effective action becomes

$$W^1 = \{2(4\pi)^{D/2} (D/2)!\}^{-1} \int d^D x \sqrt{-g} \left\{ (\gamma + \ln(\tilde{\mu}^2)) \frac{\partial^{D/2}}{\partial (is)^{D/2}} \left(e^{-is(M^2-i\epsilon)} \bar{F}(x, x; is) \right)_{s=0} - \int_0^\infty ds \ln(is) \frac{\partial^{D/2+1}}{\partial (is)^{D/2+1}} \left(e^{-is(M^2-i\epsilon)} \bar{F}(x, x; is) \right) \right\}. \quad (20)$$

We may now substitute the R -summed Schwinger-DeWitt expansion (15) in the above formula for the effective action and perform the required differentiation and integration term by term. In doing so, we use the integral identity

$$\int_0^\infty ds \ln(is) (is)^p e^{-is(M^2-i\epsilon)} = -\frac{p!}{(M^2-i\epsilon)^{p+1}} \left\{ \ln(M^2-i\epsilon) + \gamma - 1 - \frac{1}{2} - \cdots - \frac{1}{p} \right\}, \quad (21)$$

for integer values of p . This procedure finally yields

$$W^1 = \{2(4\pi)^{D/2}\}^{-1} \int d^D x \sqrt{-g} \{I_1(x) + I_2(x) + I_3(x)\}, \quad (22)$$

²We may equally well analytically continue in D instead of ν .

where

$$I_1 = -(D/2 + 1) \sum_{l=D/2+1}^{\infty} \bar{f}_l l! (M^2 - i\epsilon)^{-l+D/2} \sum_{p=0}^{D/2+1} \frac{(-1)^p}{p!(D/2 + 1 - p)!} \sum_{n=1}^{l+p-D/2-1} n^{-1} \quad (23)$$

$$I_2 = (D/2 + 1) \sum_{p=1}^{D/2+1} \sum_{l=D/2+1-p}^{D/2} \frac{(-1)^p}{p!(D/2 + 1 - p)!} \left(\gamma + \ln(M^2 - i\epsilon) - \sum_{n=1}^{l+p-D/2-1} n^{-1} \right) \times \bar{f}_l l! (M^2 - i\epsilon)^{-l+D/2}. \quad (24)$$

$$I_3 = (\gamma + \ln(\tilde{\mu}^2)) \sum_{p=0}^{D/2} \frac{(-M^2)^p}{p!} \bar{f}_{D/2-p}. \quad (25)$$

In two spacetime dimensions, the above formulae lead to the one-loop effective action

$$W_{(D=2)}^1 \approx (8\pi)^{-1} \int d^2x \sqrt{-g} \left\{ M^2 \left(\ln \left| \frac{M^2}{\tilde{\mu}^2} \right| - i\pi\theta(-M^2) \right) + \sum_{l=2}^{\infty} \left((l-1)^{-1} - l^{-1} \right) \frac{l!}{(M^2 - i\epsilon)^{l-1}} \bar{f}_l \right\}. \quad (26)$$

Similarly, in four spacetime dimensions, we get

$$I_1 = -\frac{1}{2} \sum_{l=3}^{\infty} \bar{f}_l \frac{l!}{(M^2 - i\epsilon)^{l-2}} \{ l^{-1} + 2(l-1)^{-1} - (l-2)^{-1} \} \quad (27)$$

$$I_2 = -\frac{3}{2} \bar{f}_2 - \frac{1}{2} (\gamma + \ln |M^2| - i\pi\theta(-M^2)) (2\bar{f}_2 + M^4) \quad (28)$$

$$I_3 = \frac{1}{2} (\gamma + \ln(\tilde{\mu}^2)) (M^4 + 2\bar{f}_2), \quad (29)$$

and the one-loop effective action takes the form

$$W_{(D=4)}^1 \approx -(64\pi^2)^{-1} \int d^4x \sqrt{-g} \left\{ (M^4 + 2\bar{f}_2) \left(\ln \left| \frac{M^2}{\tilde{\mu}^2} \right| - i\pi\theta(-M^2) \right) + 3\bar{f}_2 + \sum_{l=3}^{\infty} \left(l^{-1} + 2(l-1)^{-1} - (l-2)^{-1} \right) \frac{l!}{(M^2 - i\epsilon)^{l-2}} \bar{f}_l \right\}. \quad (30)$$

This is the R -summed form of the effective action. The Gaussian approximation amounts to keeping only the term multiplying M^4 in the above series. The terms involving \bar{f}_2 are required to obtain the correct trace anomaly.

The first two terms in curly brackets in Eq. (30) agree with the earlier dimensional regularization results of Parker and Toms, except for the step function term $\theta(-M^2)$ which is purely imaginary and implies particle production when M^2 becomes negative (Parker and Toms assumed $M^2 > 0$). This step function term originates from the identity $\ln(x - i\epsilon) = \ln |x| - i\pi\theta(-x)$. Within the R -summed form, therefore, the particle production takes on a very simple form, with $M^2 = 0$ being the threshold for vacuum instability, or the creation of particle pairs. It is conceivable that there are physical situations where the imaginary part of the first two terms in the above formula for the effective action very closely approximates the actual gravitational particle creation. In this paper, we do not deal with this issue further since it does not affect our results.

Note that Eq. (30) is only an asymptotic series expansion in inverse powers of M^2 , arising out of an expansion of the heat kernel which ignores, for example, terms that have essential singularities at $s = 0$. Only the first two terms (i.e. up to \bar{f}_2) are necessary for renormalization and for the correct trace anomaly. Also, these terms include the convergent infinite sum involving the scalar curvature. Therefore, the approximate effective action based on these first two terms is sufficient to indicate the non-perturbative effects coming from the infinite sum of scalar curvature terms. This is the form of the effective action that we employ.

III. RENORMALIZATION AND OBSERVABLE GRAVITATIONAL COUPLINGS

Although we are dealing with a free field theory here, the logarithmic dependence of the effective action on the curvature in Eq. (30) leads to non-trivial effects in strong curvature regions [3]. Before we go on to a discussion of such effects, it is necessary to understand the contribution of the one-loop effective action to the full gravitational action in regions of low curvature. Also, we will now consider the possibility of having multiple particle species contributing to the one-loop effective action. For particles of spin $\frac{1}{2}$ and 1, it has been shown in Ref. [8] that all terms involving R in the heat kernel can be summed in a similar manner to the spin 0 case, in a simple exponential form. We will therefore consider a generalization of Eq. (30) to the form

$$W^1 = -\hbar(64\pi^2)^{-1} \sum_i n_i \int d^4x \sqrt{-g} \{ (M_i^4 + p_i \bar{f}_{2i}) \ln | M_i^2 / \tilde{\mu}_i^2 | + q_i \bar{f}_{2i} + \dots \}, \quad (31)$$

where we have inserted arbitrary, species-dependent coefficients n_i , p_i and q_i , and a factor of \hbar is now made explicit. The imaginary term is not shown because we are interested here in the part of the effective action that corresponds to vacuum polarization. In the low curvature limit considered in this section, we can assume that $M_i^2 = m_i^2 + \bar{\xi}R > 0$, so there is no imaginary term. In later sections where M_i^2 can be negative but the curvature is very small with respect to the Planck scale, the created particles make a negligible contribution to the classical matter already present in the Robertson-Walker universe under consideration. The terms of higher order in the curvature correspond to the asymptotic series sum in Eq. (30) and do not appear in Eq. (31). For higher spin fields, the heat kernel (and the Green's function) generally has a matrix structure. In evaluating the effective action in such cases, one performs an additional trace over all internal indices. It will be understood that such a trace has been carried out before arriving at Eq. (30). \bar{f}_2 will be understood to mean the trace of the modified second Schwinger-DeWitt coefficient. The values of species-dependent coefficients for spin 1/2 are $\bar{\xi} = 1/12$, $n_i = -4$, $p_i = 1/2$, and $q_i = 3/2$.

At low scalar curvature ($\bar{\xi}R \ll m^2$), one may expand the logarithm in Eq. (31) in powers of R . Noting that \bar{f}_{2i} can be expressed as the linear combination

$$\bar{f}_{2i} = a_i \square R + b_i R_{\alpha\beta} R^{\alpha\beta} + c_i R_{\alpha\beta\gamma\delta} R^{\alpha\beta\gamma\delta}, \quad (32)$$

the leading terms in the 1-loop effective action then give

$$W^1 \simeq -\hbar(64\pi^2)^{-1} \sum_i n_i \int d^4x \sqrt{-g} \left\{ m_i^4 \ln(m_i^2 / \tilde{\mu}_i^2) + m_i^2 \bar{\xi}_i R (1 + 2 \ln(m_i^2 / \tilde{\mu}_i^2)) \right. \\ \left. + \bar{\xi}_i^2 R^2 (3/2 + \ln(m_i^2 / \tilde{\mu}_i^2)) + (b_i R_{\alpha\beta} R^{\alpha\beta} + c_i R_{\alpha\beta\gamma\delta} R^{\alpha\beta\gamma\delta}) (p_i \ln(m_i^2 / \tilde{\mu}_i^2) + q_i) + \dots \right\}, \quad (33)$$

In the above expression, we have allowed for different renormalization points characterized by the different mass scales $\tilde{\mu}_i$. Changing these mass scales give rise to terms that can be absorbed into the bare gravitational action, as will be discussed below. However, one can still remove the $\tilde{\mu}_i$ -dependence of the full effective action by using our *knowledge* of the observed gravitational coupling constants. To be precise, consider the bare gravitational action

$$W_g = \int d^4x \sqrt{-g} \{ (\kappa + \delta\kappa)(R - 2(\Lambda + \delta\Lambda)) + (\alpha_1 + \delta\alpha_1)R^2 + (\alpha_2 + \delta\alpha_2)R_{\mu\nu}R^{\mu\nu} \\ + (\alpha_3 + \delta\alpha_3)R_{\mu\nu\gamma\delta}R^{\mu\nu\gamma\delta} \} \quad (34)$$

where the counterterms are

$$\begin{aligned} \delta\Lambda &= -(128\pi^2\kappa)^{-1} \hbar \sum_i n_i m_i^4 \ln(\mu_1^2 / \tilde{\mu}_i^2) \\ \delta\kappa &= (32\pi^2)^{-1} \hbar \sum_i n_i m_i^2 \bar{\xi}_i \ln(\mu_2^2 / \tilde{\mu}_i^2) \\ \delta\alpha_1 &= (64\pi^2)^{-1} \hbar \sum_i n_i \bar{\xi}_i^2 \ln(\mu_3^2 / \tilde{\mu}_i^2) \\ \delta\alpha_2 &= (64\pi^2)^{-1} \hbar \sum_i n_i b_i p_i \ln(\mu_4^2 / \tilde{\mu}_i^2) \\ \delta\alpha_3 &= (64\pi^2)^{-1} \hbar \sum_i n_i c_i p_i \ln(\mu_5^2 / \tilde{\mu}_i^2). \end{aligned} \quad (35)$$

$\mu_{1,2,3,4,5}$ are arbitrary constants of dimension mass, and the $\tilde{\mu}_i$ -dependence of the counterterms is required, following [3], to cancel the $\tilde{\mu}_i$ -dependence in the 1-loop effective action³. Adding Eqs. (33) and (34) we obtain the full effective action at low curvatures, as

$$W \equiv W_g + W_1 = \int d^4x \sqrt{-g} \left\{ -2\kappa_o \Lambda_o + \kappa_o R + \alpha_{1o} R^2 + \alpha_{2o} R_{\alpha\beta} R^{\alpha\beta} + \alpha_{3o} R_{\alpha\beta\gamma\delta} R^{\alpha\beta\gamma\delta} + \dots \right\}, \quad (36)$$

where the subscript o refers to the observed gravitational constants at low curvatures. These are combinations of the bare and induced constants, independent of $\tilde{\mu}_i$, and given by

$$\begin{aligned} -2\kappa_o \Lambda_o &= \Lambda - \hbar(64\pi^2)^{-1} \sum_i n_i m_i^4 \ln(m_i^2/\mu_1^2) \\ \kappa_o &= \kappa - \hbar(32\pi^2)^{-1} \sum_i n_i m_i^2 \bar{\xi}_i \left(\ln(m_i^2/\mu_2^2) + \frac{1}{2} \right) \\ \alpha_{1o} &= \alpha_1 - \hbar(64\pi^2)^{-1} \sum_i n_i \bar{\xi}_i^2 \left(\ln(m_i^2/\mu_3^2) + \frac{3}{2} \right) \\ \alpha_{2o} &= \alpha_2 - \hbar(64\pi^2)^{-1} \sum_i n_i b_i (p_i \ln(m_i^2/\mu_4^2) + q_i) \\ \alpha_{3o} &= \alpha_3 - \hbar(64\pi^2)^{-1} \sum_i n_i c_i (p_i \ln(m_i^2/\mu_5^2) + q_i) \end{aligned} \quad (37)$$

Note that one can always absorb the dependence of the observed constants on the μ_i 's into the bare constants. We thus have some freedom in shifting terms within the above equations. However, as already stated, we may, in principle, use our knowledge of Λ_o , κ_o etc. in Eq. (36) at *low curvature* to explore the theory in regions of high curvature. Indeed, the full effective action in regions of high curvature now depends only on the observed values of the gravitational coupling constants at *low curvature*, on the physical particle masses m_i and on the values of $\bar{\xi}_i$ (these are fixed for higher spin fields). No other parameters enter into the effective action. To see this, we add Eqs. (31) and (34), use Eq. (35) to substitute for the counterterms, and finally use Eq. (37) to eliminate the five mass scales in favor of the observed constants. In this procedure, the $\tilde{\mu}_i$ dependence in Eq. (31) and the μ_i dependence in Eq. (37) cancel the corresponding dependences in the counterterms of Eq. (35). Then the full effective action below threshold is given by

$$\begin{aligned} W \equiv W_g + W^1 &= \int d^4x \sqrt{-g} \left\{ -2\kappa_o \Lambda_o - \hbar \frac{1}{64\pi^2} \sum_i n_i m_i^4 \ln \left| \frac{M_i^2}{m_i^2} \right| \right. \\ &\quad + \left(\kappa_o + \hbar \frac{1}{64\pi^2} \sum_i n_i m_i^2 \bar{\xi}_i \left(1 - 2 \ln \left| \frac{M_i^2}{m_i^2} \right| \right) \right) R \\ &\quad - \hbar \frac{1}{64\pi^2} \sum_i n_i p_i \ln \left| \frac{M_i^2}{m_i^2} \right| f_{2i} + \left(\alpha_{1o} + \hbar \frac{3}{128\pi^2} \sum_i n_i \bar{\xi}_i^2 \right) R^2 \\ &\quad \left. + \alpha_{2o} R_{\alpha\beta} R^{\alpha\beta} + \alpha_{3o} R_{\alpha\beta\gamma\delta} R^{\alpha\beta\gamma\delta} + \dots \right\}, \end{aligned} \quad (38)$$

where f_{2i} is given by

$$p_i f_{2i} = p_i \bar{f}_{2i} + \frac{1}{2} \bar{\xi}_i^2 R^2. \quad (39)$$

Here,

³In zeta function regularization, the divergent pieces of the one-loop effective action have been thrown away beforehand, which is why it is not necessary to introduce those divergences into the counterterms either (although this procedure of introducing counterterms could be bypassed in zeta-function regularization, it is necessary in other regularization schemes, such as dimensional regularization). In dimensional regularization [3], one explicitly keeps track of the divergent pieces and introduces corresponding divergences in the counterterms. Since the divergences are ultimately canceled, one finally ends up with Eq. (37) in any case.

$$\kappa_o = (16\pi G_o)^{-1}, \quad (40)$$

where G_o is Newton's gravitational constant, and Λ_o is the usual cosmological constant.

Eq. (38) is a new result, relating behavior at high curvatures to values of the gravitational coupling constants at low curvatures. For scalar fields, $\bar{\xi}$ is the only undetermined parameter in the effective action. For higher spins, the corresponding parameters have fixed values. We emphasize again that terms involving \bar{f}_3 and higher, omitted in Eq. (38), constitute an asymptotic expansion in inverse powers of M^2 and are therefore not necessarily expected to be physically significant. The terms retained in Eq. (38) are the minimal set of terms necessary for renormalization and incorporate the sum of scalar curvature terms in the propagator. It is readily checked that Eq. (36) constitutes the first few terms in the low-scalar-curvature limit ($|\bar{\xi}R| \ll m^2$) of Eq. (38).

In subsequent Sections, we consider the gravitational field equations for a single scalar field, as derived from Eq. (38), and their consequences. Comparison of Eqs. (31) and (30) gives, for scalar fields, $n_i = 1, p_i = 2, q_i = 3$. In Section V, we study the case of constant curvature spacetimes. In later sections, we generalize the investigation to Robertson-Walker universes containing matter and radiation. In the next Section, we clarify the usage of the terms "perturbative" and "exact" in this paper.

IV. MEANING OF EXACT AND PERTURBATIVE SOLUTIONS

In the previous section we derived the effective action, Eq. (38), appropriate to the R -summed propagator. All terms multiplied by \hbar in Eq. (38) will be called "quantum-vacuum" terms, also referred to as one-loop terms, because they arise after vacuum fluctuations of the field have been integrated out in a path-integral formulation of the theory. However, note that factors of \hbar must also be included in the argument of the logarithmic terms for dimensional reasons. Indeed, one has

$$\ln |M^2/m^2| = \ln |(m^2 + \hbar^2 \bar{\xi}R)/m^2|. \quad (41)$$

An approach that is completely perturbative in \hbar would then involve expanding out the logarithmic terms. However, the factor of \hbar^2 appearing in the above equation has its origins in the generalized Klein-Gordon equation

$$\left(-\square + \frac{m^2}{\hbar^2} + \xi R\right)\phi = 0, \quad (42)$$

whose solutions contribute to the *tree-level* effective action, as opposed to the quantum-vacuum or one-loop effective action. That is, the \hbar^2 factor above does not arise from integrating out vacuum fluctuations. Furthermore, the quantity m^2/\hbar^2 is the square of the inverse Compton wavelength of the field, and need not be large relative to the curvature scalar. Therefore, it is reasonable to regard the logarithmic terms as non-perturbative when expanding in \hbar . It is convenient to avoid explicitly inserting factors of \hbar in the arguments of logarithmic terms (more generally, in any term which contains M^2), with the understanding that the mass of the field is interpreted as an inverse Compton wavelength.

A *perturbative* analysis in \hbar , as used in Section VI of this paper, therefore treats only the quantum-vacuum corrections in a perturbative fashion, while keeping the logarithmic terms intact. It is not inconsistent to do so, since it defines a regime in which the semiclassical corrections to the effective action are much smaller than the tree-level terms involving Λ_o and κ_o , yet in which the scalar curvature is allowed to be of the same order as the square of the inverse Compton wavelength. On the other hand, an *exact* analysis, as used in Section V below, treats even the quantum corrections in an exact fashion.

The reason we carry out both perturbative and exact analyses is as follows. Exact solutions play a significant role when the perturbative analysis breaks down (as signaled by a rapid growth in the contributions of quantum corrections to the metric). In order to obtain an understanding of the full dynamics of the metric, it is therefore necessary to construct both perturbative and exact solutions to the semiclassical Einstein equations.

It is well-known [15] that semiclassical equations of motion can be perturbatively reduced in a manner such that the resulting equations only admit solutions that are perturbative in \hbar . It has been further argued that such solutions are the only physically viable solutions of the full semiclassical equations since they do not exhibit runaway behavior in the classical limit.

However, in Section V, we argue for the physical significance of our exact solutions. This argument is based on two observations. First, owing to the presence of a mass scale in the theory, \hbar explicitly enters into the semiclassical equations only via the dimensionless ratio $r \equiv m^2/m_{Pl}^2$. This ratio is not necessarily small, although perturbation theory assumes that it is. Thus, there could be physical effects at large r , not encountered in perturbation theory.

Secondly, we will find exact solutions that cannot be expanded in \hbar and have a well-defined limit as $r \rightarrow 0$, i.e. they do not possess runaway behavior in the classical limit. Such solutions must therefore be regarded as physical solutions.

For these reasons, we believe that exact solutions that do not arise from perturbative reduction must be included in a complete analysis of solutions of the semiclassical Einstein equations, at least when a mass scale is present in the theory.

V. EXACT VACUUM DE SITTER SOLUTIONS

In this section, we will consider exact solutions to the equations of motion specialized to de Sitter spacetime. These equations simplify considerably for spacetimes of constant curvature. This simplification allows us to include in the effective action terms involving \bar{f}_2 and R^2 .

As we shall see, there is a rich variety of constant curvature de Sitter solutions, with the scalar curvature being highly sensitive to the value of $\bar{\xi}$. We will argue that these solutions are physically viable although they do not appear in the perturbative reduction approach.

Consider, therefore, the effective action of Eq. (38), specialized to a single scalar field with mass m and curvature coupling ξ :

$$W = \int d^4x \sqrt{-g} \left\{ -2\kappa_o \Lambda_o - \hbar \frac{1}{64\pi^2} m^4 \ln \left| \frac{M^2}{m^2} \right| + \left(\kappa_o + \hbar \frac{1}{64\pi^2} m^2 \bar{\xi} \left(1 - 2 \ln \left| \frac{M^2}{m^2} \right| \right) \right) R - \hbar \frac{1}{32\pi^2} \ln \left| \frac{M^2}{m^2} \right| f_2 + \hbar \frac{3}{128\pi^2} \bar{\xi}^2 R^2 \right\}, \quad (43)$$

where we have assumed that the constants α_{1o} , α_{2o} and α_{3o} are negligibly small⁴.

One may now use Eqs. (B1-B9) of Appendix B to obtain the equations of motion resulting from the variation of Eq. (43). When specialized to a constant curvature maximally symmetric spacetime, in which

$$R_{\mu\nu\alpha\beta} = \frac{R}{12} (g_{\mu\alpha} g_{\nu\beta} - g_{\nu\alpha} g_{\mu\beta}), \quad (44)$$

these equations yield a single algebraic equation satisfied by the scalar curvature R :⁵

$$2\kappa_o(4\Lambda_o - R) = -\frac{\hbar}{16\pi^2} \left\{ m^4 \ln \left| \frac{M^2}{m^2} \right| \left(1 + \frac{\bar{\xi} R}{m^2} \right) - \frac{1}{2} m^2 \bar{\xi} R \left(1 + \frac{m^2}{M^2} \right) - \bar{\xi}^2 R^2 \frac{m^2}{M^2} - \frac{1}{2} \bar{\xi} \frac{R^3}{M^2} \left(\bar{\xi}^2 - \frac{1}{1080} \right) \right\}. \quad (45)$$

Note that we recover Starobinsky inflation by first taking $\Lambda_o \rightarrow 0$ and $m \rightarrow 0$, and then taking the limit $\bar{\xi} \rightarrow 0$. The resulting solution has scalar curvature $R = 69120 \pi^2 \kappa_o \hbar^{-1}$, in agreement with Starobinsky's results [16]. The Starobinsky solution is non-analytic in \hbar and is not well-defined in the limit $\hbar \rightarrow 0$. The existence of such solutions has motivated arguments in favor of the perturbative reduction scheme [15], which discards such solutions in a self-consistent manner.

⁴For the purposes of this section, it is actually sufficient to assume that terms involving α_{1o} , α_{2o} and α_{3o} combine to yield $\alpha_o f_2$ + negligible contributions, where α_o is some constant, because the variation of $\int d^4x \sqrt{-g} f_2$ vanishes in a constant curvature spacetime.

⁵The right-hand-side (RHS) of Eq. (45) gives the trace of a stress-tensor in de Sitter space which is not the same as the stress-tensor for the Bunch-Davies vacuum state. The stress-tensor on the RHS of Eq. (45) corresponds to a different state and is defined by variation of W . The leading terms of the stress-tensor agree with those arising from the Gaussian approximation of Bekenstein and Parker [9], which is known to be a good approximation in de Sitter space, particularly for closely spaced points as are used in defining the stress tensor. The additional term, $(1/2)(1/1080)\bar{\xi}(R^3/M^2)$ in Eq. (45) yields the correct trace anomaly. Furthermore, this stress-tensor is conserved, and vanishes in flat spacetime ($R = 0$). The RHS of Eq. (45) diverges at $M^2 = m^2 + \bar{\xi}R = 0$. Similar divergences also occur in the stress tensor in the Bunch-Davies vacuum state in de Sitter space, which diverges at $m^2 + (\xi + n(n+3)/12)R = 0$, where n is a non-negative integer.

However, such arguments weaken in the presence of an additional mass scale m in the theory. To see this, consider Eq. (45) rewritten in terms of the dimensionless variables

$$y = \frac{R}{m^2} \quad (46)$$

$$r = \frac{\hbar m^2}{16\pi\kappa_o}. \quad (47)$$

Recall that m refers to the inverse Compton wavelength of the particle, so y and r are indeed dimensionless. In terms of the actual mass of the particle, r is given by

$$r = \frac{m_{\text{actual}}^2}{m_{Pl}^2}, \quad (48)$$

where $m_{Pl} = \sqrt{16\pi\kappa_o\hbar}$.

Eq. (45) then takes the form

$$(1 + \bar{\xi}y) \ln |1 + \bar{\xi}y| - \frac{\bar{\xi}y}{1 + \bar{\xi}y} \left\{ 1 + \frac{3}{2}\bar{\xi}y + \frac{1}{2}y^2 \left(\bar{\xi}^2 - \frac{1}{1080} \right) \right\} = \frac{2\pi}{r} \left(y - \frac{4\Lambda_o}{m^2} \right). \quad (49)$$

The solution for y is a function of three dimensionless parameters: r , $\bar{\xi}$ and Λ_o/m^2 . In a perturbative reduction approach, r is regarded as a small parameter and the solution for y is constrained to be an analytic function of r . However, it is plausible that the limit $\hbar \rightarrow 0$ does not imply $r \rightarrow 0$, i.e. that the mass m is rescaled in such a manner that r stays constant (or roughly constant) as $\hbar \rightarrow 0$. For example, in string theory, one would expect that all masses (including the Planck mass m_{Pl}) are generated by a single scale (the string scale), in which case the dimensionless quantity r would be independent of \hbar . In the absence of knowledge of the precise nature of a fundamental unified theory, it is therefore prudent to consider the possibility that the parameter r is some finite quantity, not necessarily small, and to treat it in a non-perturbative fashion⁶. In subsection B, we give a further justification for the physical validity of solutions that arise without expanding in r . Namely, we find that for $\bar{\xi} < 0$, these solutions have a well-defined classical limit as \hbar (or r) $\rightarrow 0$.

We now consider numerical solutions to the algebraic equation (49). This equation, in general, has solutions with both positive and negative scalar curvature. We will, however, focus on the positive scalar curvature solutions ($y > 0$), corresponding to an inflating de Sitter universe. Figs. 1 and 2 are plots of the left hand side (LHS) and right hand side (RHS) of Equation (49), as functions of y , for various values of the three parameters r , $\bar{\xi}$ and Λ_o/m^2 . The point(s) of intersection of the LHS and RHS correspond to solutions for y . These plots are convenient ways of identifying the solution space because the LHS depends solely on the parameter $\bar{\xi}$, while the RHS is a linear function of y , with slope given by r , and intercept given by Λ_o/m^2 . In all plots, therefore, the straight line is the RHS of Eq. (49). Increasing the value of r will decrease the slope of the straight line. Increasing Λ_o will shift the straight line up. It is convenient to consider two ranges of values of $\bar{\xi}$ that give qualitatively different behavior of the LHS of Eq. (49). These are: a) $\bar{\xi} > 0$, and b) $\bar{\xi} < 0$.

We will find that there exist solutions with non-zero scalar curvature, even if $\Lambda_o = 0$. For $\bar{\xi} > 0$, the most interesting solutions of this type exist for values of $\bar{\xi}$ very close to $(1080)^{-\frac{1}{2}}$. For other values of $\bar{\xi} > 0$, there are either no solutions or solutions for which the scalar curvature is of order m_{Pl}^2 , which may thus be unphysical.

For $\bar{\xi} < 0$, we find that there exist solutions with $R \simeq -m^2/\bar{\xi}$, for a large range of values of $\bar{\xi}$ and r , and for small and large values of Λ_o/m^2 . These solutions are of greater interest for the purposes of this paper, and the reader may safely skip directly to subsection B.

A. Solutions with $\bar{\xi} > 0$

For $\bar{\xi} > 1080^{-1/2}$ and $\Lambda_o = 0$, the only solution to Eq. (49) is the trivial solution $y = 0$, because, for $y > 0$, the LHS is always negative, while the RHS is always positive. However, addition of a non-zero value of Λ_o allows the RHS

⁶Different arguments for the physical significance of solutions that do not arise from perturbative reduction have been given by Wai-Mo Suen [17].

to take negative values, and leads to a non-trivial solution with a value of y slightly lower than the classical value $4\Lambda_o/m^2$. The deviation from classical behavior will typically be very small due to the extreme flatness of the LHS graph near the origin.

As one lowers the value of $\bar{\xi}$ towards $(1080)^{-1/2}$, the LHS acquires a local maximum (Fig. 1). The position of this maximum is very sensitive to the value of $\bar{\xi}$ when $\bar{\xi}$ is close to the value $(1080)^{-1/2}$. For large values of r ($r = 10$ in the figure), a non-trivial intersection with the RHS graph is now possible, with y -values ranging from about a hundred to extremely large values, depending on the precise values of $\bar{\xi}$ and r . The presence of a non-zero Λ_o term would shift the RHS graph down and increase the value of y even further.

When $\bar{\xi} = (1080)^{-1/2} = 0.03042\dots$, the non-trivial intersection point of the two graphs will occur at an extremely large value of y , for typical values of r . One may obtain an analytical estimate by considering an approximation to Eq. (49) for large y , after setting $\bar{\xi} = (1080)^{-1/2}$. This gives

$$\ln \frac{y}{\sqrt{1080}} = \frac{2\pi}{r} \sqrt{1080} + \frac{3}{2}. \quad (50)$$

For $r = 1$ ($m = m_{Pl}$), the above equation implies a value of y approximately equal to about 10^{91} . This value *increases* as r *decreases* (i.e. by decreasing m and holding m_{Pl} constant) and vice-versa. However $R = m^2 y = m_{Pl}^2 r y$ will acquire a minimum value for some $r > 1$. Also, addition of a Λ_o term tends to decrease the value of y and, consequently, R .

For $0 < \bar{\xi} < (1080)^{-1/2}$, there is a non-trivial solution with an extremely large value of y . An analytic approximation to Eq. (49) can be made once more, after noting that the term involving y^2 in the LHS is now the dominant term (this term vanishes when $\bar{\xi} = (1080)^{-1/2}$). Thus we obtain, in this regime, with zero cosmological constant,

$$y = \frac{4\pi}{r} \left(\frac{1}{1080} - \bar{\xi}^2 \right)^{-1}. \quad (51)$$

y therefore scales linearly with r^{-1} . However, the scalar curvature itself is essentially independent of m in this regime, and is given by

$$R = 4\pi m_{Pl}^2 \left(\frac{1}{1080} - \bar{\xi}^2 \right)^{-1}. \quad (52)$$

The two equations above predict that y (or R) will decrease as $\bar{\xi}$ decreases. This behavior is borne out by numerical study. However, when $\bar{\xi}$ is extremely small, $\bar{\xi}y$ can become small, and the large- $\bar{\xi}y$ approximation breaks down. For very small values of $\bar{\xi}$, the solution for y then increases with decreasing $\bar{\xi}$, giving $y \rightarrow \infty$ as $\bar{\xi} \rightarrow 0^+$, as expected from Eq. (49).

To summarize, for $\bar{\xi} > 0$ and $\Lambda_o = 0$, non-zero solutions for constant scalar curvature occur for $\bar{\xi}$ values very close to $(1080)^{-1/2}$ (this corresponds to the curvature coupling ξ being very close to the conformal fixed point $\xi = 1/6$, because $(1080)^{-1/2}$ is a small number). Such solutions also occur for $\bar{\xi} = (1080)^{-1/2}$; however, in this case, the curvature is typically many orders of magnitude greater than Planck size, and may thus be unphysical.

B. Solutions with $\bar{\xi} < 0$

For $\bar{\xi} < 0$, the LHS of Eq. (49) becomes singular at $y = -\bar{\xi}^{-1}$. This value of y becomes an exact solution to Eq. (49) in the ‘‘classical’’ limit $r \rightarrow 0$, as can be seen by letting $y = -\bar{\xi}^{-1} + \epsilon(r)$ in Eq. (49), and showing that $\epsilon(r) \rightarrow 0$ as $r \rightarrow 0$. This fact constitutes another argument against the perturbative reduction scheme in this case, because the scalar curvature does not exhibit runaway behavior in the classical limit. As we shall see, most solutions with $r < 1$, will lie very close to the value $y = -\bar{\xi}^{-1}$. Significant deviations from this value will occur only for very large values of r , or when a non-zero Λ_o term is present.

Fig. 2 is a plot of the LHS and RHS of Eq. (49) with representative values $\bar{\xi} = -0.03$ and $\Lambda_o = 0$. An exaggerated value of $m = 4m_{Pl}$ is used to fully display the graph. However, as we will see, the solution for y is largely insensitive to the precise values of $\bar{\xi}$ and r .

The straight line LHS graph intersects the RHS graph at a y -value very slightly larger than $-\bar{\xi}^{-1}$ ($= 33.3\dots$ in this case). The corresponding scalar curvature is given by $R \simeq m^2 \bar{\xi}^{-1}$. The steep vertical ascent of the LHS graph near the value $y = -\bar{\xi}^{-1}$ implies that the solution for y is not very sensitive to the precise value of r (note that decreasing r increases the slope of the straight line, giving a solution even closer to the value $\bar{\xi}^{-1}$). For most values of r , except

for exceptionally large values, we have a solution at $R = -m^2\bar{\xi}^{-1}$ plus a small correction. The presence of a Λ_o term has the effect of shifting down the RHS graph, leading to larger values of the scalar curvature. However, in this case, a second solution will appear with $y < -\bar{\xi}^{-1}$, the y -value being very close to the classically expected value $4\Lambda_o/m^2$, for a small cosmological constant. As the cosmological constant is increased to large values this second solution will now approach $y = -\bar{\xi}^{-1}$, while the first solution now corresponds to the classically expected large value of y . The solution $y \simeq -\bar{\xi}^{-1}$ is therefore fairly robust; it exists for large ranges of the parameter r and for both small and large values of Λ_o . Numerical investigation shows that such a solution also exists for a large range of values of $\bar{\xi}$.

It should be noted that a y value slightly larger than $-\bar{\xi}^{-1}$ corresponds to a small negative value of M^2 , and therefore the effective action evaluated on such a solution acquires a small imaginary part giving rise to a small rate of particle production. In the regime we consider in this paper, the effects of this particle production are negligible.

The qualitative behavior of the LHS of Eq. (49) for $\bar{\xi} = -(1080)^{-\frac{1}{2}}$ is very similar to the behavior for $\bar{\xi} = -1$, and quite insensitive to the precise value of r , as in the previous case. The solution will now be very close to $y = -\bar{\xi}^{-1} \simeq 32.86\dots$, implying that the scalar curvature is about an order of magnitude larger than m^2 , for a large range of values of m . Again, this is a robust solution as discussed earlier.

To summarize, for $\bar{\xi} < 0$, we find physically reasonable values (in the sense that they could be small with respect to m_{Pl}^2) of the scalar curvature, approximately given by

$$R \simeq -\frac{m^2}{\bar{\xi}} = \bar{m}^2 \quad (53)$$

for a large range of values of r , $\bar{\xi}$ and Λ_o . The approximation in Eq. (53) breaks down if $\Lambda_o = 0$ and $r \gg 1$, in which case the only solution corresponds to an extremely large scalar curvature ($R \gg m_{Pl}^2$) whose precise value depends on r and $\bar{\xi}$. This large R solution will give rise to a large imaginary contribution to the effective action, and so one expects copious amounts of particle production to occur, which could, in turn, bring the scalar curvature down to reasonable values. This would be consistent with a gravitational Lenz's law mechanism [1,18,19]. We do not address this issue here. Instead, we now turn to a perturbative analysis of the semiclassical Einstein equations.

VI. THE GROWTH OF QUANTUM CORRECTIONS TO THE SCALAR CURVATURE

In this section, we will analyze, the effect of logarithmic curvature terms in the effective action on a Robertson-Walker cosmology. We analyze this effect in two ways, valid for spatially open, closed and flat models. First, we consider a universe with mixed matter and radiation and assume that the scalar curvature is slowly varying so that its derivatives can be ignored. This analysis shows that perturbative (as defined in Sec. IV) quantum corrections to the scalar curvature can sharply increase in magnitude near a time t_j that is determined by m and $\bar{\xi}$. In particular, the existence of an ultralight mass in the theory can lead to significant quantum effects close to the present time. Since the background classical scalar curvature is decreasing, the effect of quantum corrections is to prevent the scalar curvature from decreasing further. However, as quantum corrections become more and more significant, perturbation theory breaks down and cannot be relied upon to give the full behavior of the scalar curvature. We then carry out a second analysis of the behavior of the scalar curvature for all times after t_j , without using perturbation theory. This second analysis indeed reveals that, for $t > t_j$, the scalar curvature tends to decrease extremely slowly, ultimately approaching a constant value. The analysis thus displays consistency with the original assumption of slowly varying scalar curvature.

In Section VII, we will use the behavior of the scalar curvature to construct a model universe in which a matter-dominated cosmology transits to a mildly inflating de Sitter cosmology at the time t_j .

A. Quantum Corrections to the scalar curvature

In this subsection, we will consider a classical Robertson-Walker cosmology with mixed matter and radiation, and treat the quantum effects involving logarithmic curvature terms in a perturbative fashion (recall the discussion in Section IV, which shows why an expansion of the logarithm itself is not appropriate in a perturbative treatment of quantum-vacuum terms). The universe will deviate from classical behavior when the quantum effects become sufficiently large. The essential idea is to allow for the possibility of quantum effects being significant at the present time. We will find that this is possible if there exist very light mass fields with $\bar{\xi} < 0$.

Our starting point for the analysis here is the effective action of Eq. (43). Variation of this effective action, specialized to a Robertson-Walker metric, will generally yield terms involving derivatives of the scalar curvature R , in addition to the terms of Eq. (45). In this subsection, we assume that terms involving derivatives of the scalar curvature are negligible. We will find that, for light mass fields ($m \ll m_{Pl}$), this assumption is justified because derivatives of the scalar curvature remain small until the magnitude of the quantum-vacuum contribution to the scalar curvature itself becomes comparable to the classical contribution to the scalar curvature. Beyond this point, the perturbative analysis breaks down. In the next subsection, we carry out an exact analysis, valid for $t > t_j$.

Although we ignore derivatives of the scalar curvature when carrying out the variation of Eq. (43), the resulting semiclassical Einstein equations differ from Eq. (45) in two important respects. First, the fact that the Robertson-Walker universe has fewer symmetries than de Sitter space gives additional terms in the semiclassical Einstein equations. Secondly, we will include a classical stress tensor source representing mixed matter and radiation. We also set $\Lambda_o = 0$. The trace of the semiclassical Einstein equations, expressed in terms of dimensionless variables, then takes the form of a simple generalization of Eq. (49):

$$\begin{aligned} r(1 + \bar{\xi}y) \ln |1 + \bar{\xi}y| - r \frac{\bar{\xi}y}{1 + \bar{\xi}y} \left\{ 1 + \frac{3\bar{\xi}y}{2} + \frac{1}{2}y^2 \left(\bar{\xi}^2 - \frac{1}{1080} \right) + v \right\} \\ = 2\pi \left(y + \frac{T}{2m^2\kappa_o} \right), \end{aligned} \quad (54)$$

where T is the trace of the classical stress tensor, and v is a quantity which vanishes in de Sitter space:

$$v = \frac{1}{180m^4} \left(\frac{1}{4}R^2 - R_{\mu\nu}R^{\mu\nu} \right). \quad (55)$$

All quantum contributions are grouped in the LHS of Eq. (54), while its RHS contains classical terms.

Consider now the full semiclassical Einstein equations with a classical stress tensor source representing mixed matter and radiation,

$$G^{\mu\nu} = \frac{1}{2\kappa_o} \left(\left(\rho_m + \frac{4}{3}\rho_r \right) u^\mu u^\nu + \frac{1}{3}\rho_r g^{\mu\nu} \right) + \mathcal{O}(\hbar), \quad (56)$$

where ρ_m and ρ_r represent the matter and radiation energy densities, respectively, and $\mathcal{O}(\hbar)$ represents the quantum contributions. The equation above implies

$$y \equiv \frac{R}{m^2} = \frac{\rho_m}{2\kappa_o m^2} + \frac{R_Q}{m^2}, \quad (57)$$

$$v = -\frac{(\rho_m + (4/3)\rho_r)^2}{960m^4\kappa_o^2} + \mathcal{O}(\hbar), \quad (58)$$

where R_Q , as defined by Eq. (57), is of order \hbar . In a treatment perturbative in \hbar , we replace y and v in the LHS of Eq. (54) by their classical values using the above equations, because the factor r is of order \hbar . This treatment is valid as long as the LHS of Eq. (54) is small with respect to the term $\pi T/(m^2\kappa_o)$ in the RHS. In the RHS of Eq. (54) we keep the quantum-vacuum contribution to y as well (i.e. the term R_Q/m^2). Furthermore, in a Robertson-Walker cosmology with metric

$$ds^2 = -dt^2 + a(t)^2 \left(\frac{dr^2}{1 - kr^2} + r^2 d\Omega^2 \right), \quad (59)$$

where $k = -1, +1$ and 0 denote spatially open, closed and flat universes respectively, we have $\rho_m \propto a^{-3}$ and $\rho_r \propto a^{-4}$. It is then more convenient to express y and v in terms of the present matter and radiation densities ρ_{m_0} and ρ_{r_0} , and the redshift z . We therefore introduce new dimensionless variables d_m and d_r , given by

$$e^{-d_m} \equiv \frac{\rho_{m_0}}{m_{Pl}^2 \kappa_o}, \quad (60)$$

$$e^{-d_r} \equiv \frac{\rho_{r_0}}{m_{Pl}^2 \kappa_o}, \quad (61)$$

and the redshift z given by

$$1 + z = \frac{a_0}{a}, \quad (62)$$

where a_0 is the scale factor at the present time. Furthermore, owing to the fact that we will study the effect of very light masses, we also redefine the ratio m^2/m_{Pl}^2 :

$$r = e^{-S}. \quad (63)$$

Eq. (54) can now be rewritten by substituting for y and v using Eqs. (57) and (58) with the redefined variables of Eqs. (60), (60), (62) and (63) above. The resulting equation, correct to leading order in \hbar , gives an expression for the quantum correction to the scalar curvature, R_Q , as a function of redshift. Dividing by $R_{cl} = \rho_m/(2\kappa_o)$, we obtain

$$\begin{aligned} \frac{R_Q}{R_{cl}} &\equiv \frac{R_Q}{\rho_m/(2\kappa_o)} \\ &= \frac{e^{d_m-2S}}{\pi(1+z)^3} \left\{ \left(1 + \frac{1}{2}\bar{\xi}(1+z)^3 e^{S-d_m} \right) \ln \left| 1 + \frac{1}{2}\bar{\xi}(1+z)^3 e^{S-d_m} \right| \right. \\ &\quad - \frac{1}{2} \frac{\bar{\xi}(1+z)^3 e^{S-d_m}}{1 + \frac{1}{2}\bar{\xi}(1+z)^3 e^{S-d_m}} \left\{ 1 + \frac{3}{4}\bar{\xi}(1+z)^3 e^{S-d_m} + \frac{1}{8} \left(\bar{\xi}^2 - \frac{1}{108} \right) (1+z)^6 e^{2(S-d_m)} \right. \right. \\ &\quad \left. \left. - \frac{1}{480}(1+z)^7 e^{2S-d_r-d_m} - \frac{1}{960}(1+z)^8 e^{2(S-d_r)} \right\} \right\}. \end{aligned} \quad (64)$$

We wish to find the redshift ranges for which the quantum contribution to the scalar curvature is significant in comparison with the classical contribution (i.e. R_Q/R_{cl} of order 1). The values of d_r and d_m in Eq. (64) are determined by the radiation and matter energy densities at the present time. Black body radiation at a temperature of 2.726 K gives a radiation energy density $\rho_{r0} \simeq 7.81 \times 10^{-34} \text{g/cm}^3$ [20,21]. This gives a value for $d_r \simeq 288.06$. The matter density is not known to good precision. With the conservative estimates $\Omega_0 > 0.1$ for the ratio of the present matter density to the critical density, and $H_0 > 50 \text{km/(sMpc)}$ for the Hubble constant at the present time, we obtain $\rho_{m0} > 4.70 \times 10^{-31} \text{g/cm}^3$ for the matter density. This gives $d_m < 281.66$ for the exponent of Eq. (60).

For very light masses ($S > 150$), numerical investigations of the ratio R_Q/R_{cl} as a function of redshift z , using Eq. (64) with $|\bar{\xi}| \simeq 1$, reveal that there are two distinct regimes for which this ratio is close to or larger than 1. The first such regime occurs at extremely high redshifts ($z > 10^{26}$), close to the GUT scale. [In the standard cosmology, the Planck era occurs at a redshift of about 10^{31} , while the GUT era sets in at a redshift of about 10^{26} .] It is expected that quantum effects would play a significant role at such high redshifts. The *second*, unexpected regime for which the quantum-vacuum terms become large occurs at relatively low redshifts. This second regime exists only for $\bar{\xi} < 0$, and occurs when the factor $1 + (1/2)\bar{\xi}(1+z)^3 e^{S-d_m}$ in Eq. (64) approaches zero. This corresponds to values of z near a redshift z_j given by

$$(1 + z_j)^3 = -2\bar{\xi}^{-1} e^{d_m-S}. \quad (65)$$

In between these early and late regimes, the quantum contribution to the scalar curvature is extremely small and slowly varying, and the evolution of the universe is well-approximated by its classical evolution.

Numerical investigation of the behavior of the ratio R_Q/R_{cl} for values $\bar{\xi} = -1$ and $d_m \simeq 280$, and for very light masses ($S > 150$), further reveals that in the late regime of significance of quantum vacuum terms (i.e. near $z = z_j$), the scalar curvature sharply increases as $z \rightarrow z_j$. Since z_j depends on S (from Eq. (65)), and therefore on m , the value of m dictates the value of z_j at which quantum vacuum terms can become significant. As we shall see later, an ultralight mass can lead to quantum vacuum effects becoming significant at roughly half the age of the universe. However, it is important to note that when the scalar curvature begins its rapid increase near redshift z_j , quantum effects begin to dominate and the perturbative analysis itself breaks down.

For our purposes, we will only need the result that the ratio R_Q/R_{cl} tends to rapidly increase as $z \rightarrow z_j^+$. The total scalar curvature R , which can be written as

$$R = R_{cl} \left(1 + \frac{R_Q}{R_{cl}} \right), \quad (66)$$

is thus a product of a decreasing function (R_{cl}) and an increasing function. For $z \gg z_j$, $R \simeq R_{cl}$ decreases, and as $z \rightarrow z_j^+$, the quantity R_Q/R_{cl} tends to suppress the further decrease of R .

It will be useful to have an estimate of z_j relative to the redshift at matter-radiation equality, z_{eq} . The quantity z_{eq} is defined by the condition of equality of matter and radiation energy densities:

$$\rho_{m0}(1+z_{eq})^3 = \rho_{r0}(1+z_{eq})^4. \quad (67)$$

Combining Eqs. (65), (67), (60) and (61), we get

$$\frac{1+z_j}{1+z_{eq}} = \left(\frac{2}{-\bar{\xi}}\right)^{1/3} e^{4d_m/3-d_r-S/3}. \quad (68)$$

As earlier, we suppose that $d_r \simeq 288.06$ and $d_m < 281.66$. Also, we will additionally assume that $S > 278$.⁷ With these ranges, we obtain

$$\frac{1+z_j}{1+z_{eq}} < \left(\frac{2}{-\bar{\xi}}\right)^{1/3} 5.61 \times 10^{-3}. \quad (69)$$

Thus, if $-\bar{\xi}$ is of order 1, we have $z_j \ll z_{eq}$.

It follows, for this range of masses, that the quantum corrections become significant at some time during the matter-dominated stage of the expansion. In Section VII, we derive a formula for the cosmic time t_j corresponding to the redshift z_j , for a spatially open matter-dominated universe.

To find the scalar curvature at t_j , we use Eqs. (60) and (61) to write

$$\begin{aligned} (1+z_j)^3 e^{S-d_m} &\equiv (1+z_j)^3 \frac{\rho_{m0}}{m^2 \kappa_0} \\ &= \frac{\rho_{mj}}{m^2 \kappa_0} \\ &= \frac{2R_{cl}(t_j)}{m^2}, \end{aligned} \quad (70)$$

where ρ_{mj} is the matter density at time t_j , and the last equality in the above equation follows from the classical Einstein equations. Comparing the above equation with Eq. (65) shows that

$$R_{cl}(t_j) = m^2/(-\bar{\xi}) = \bar{m}^2. \quad (71)$$

We will now carry out a second analysis, valid outside the perturbative regime, which shows that the scalar curvature indeed approaches a constant value as $z \rightarrow z_j$ (or $t \rightarrow t_j$).

B. Behavior of the scalar curvature for $t > t_j$

As t approaches t_j , the arguments of the previous subsection show that the classical scalar curvature of the matter-dominated universe approaches the value $R_j = \bar{m}^2$. We will now argue that the scalar curvature does not decrease further for $t > t_j$, i.e. it saturates to a value very close to, but slightly larger than R_j . That is, we will show that there exist approximately de Sitter-like solutions to Eq. (54) for which the scalar curvature does not change significantly, although the matter density keeps decreasing, eventually approaching zero at very late times. We find that, for matter densities less than ρ_{mj} there exist de Sitter type solutions of Eq. (54) of the form

$$R = \bar{m}^2(1 - \epsilon) \quad (72)$$

such that $|\epsilon| \ll 1$, and R is an extremely slowly varying function of the matter density. We will assume throughout that the mass m is very light ($r \ll 1$), and that $-\bar{\xi}$ is positive and of order 1.

To show that Eq. (72) is indeed a solution, we substitute Eq. (72) in Eq. (54) and assume $v \ll 1$, so that one can effectively ignore v . Then Eq. (54) takes the form

$$\begin{aligned} \epsilon \ln |\epsilon| - \frac{\epsilon - 1}{\epsilon} \left\{ 1 + \frac{3}{2} + \frac{1}{2}(1 - \epsilon)^2(1 - (1080\bar{\xi}^2)^{-1}) + v \right\} = \\ \frac{2\pi}{r} \left(\frac{\epsilon - 1}{\bar{\xi}} + \frac{T}{2m^2\kappa_o} \right). \end{aligned} \quad (73)$$

⁷This assumption will be justified in the next section, where we find the value of the mass (and therefore S).

Define

$$\delta \equiv \frac{T}{2m^2\kappa_o} - \bar{\xi}^{-1} = -\frac{\rho_m}{2m^2\kappa_o} - \bar{\xi}^{-1}. \quad (74)$$

If $\rho_m = \rho_{mj}$, where ρ_{mj} is found from Eqs. (65) and (70), $\delta = 0$; and if $\rho_m = 0$, $\delta = -\bar{\xi}^{-1}$. We find that $|\epsilon|$ is always small within this range of δ values. In fact, we show that it is small for any positive value of δ . In the small $|\epsilon|$ approximation, Eq. (73) becomes

$$\epsilon^{-1} \left(-\frac{1}{2(1080)\bar{\xi}^2} + v \right) = \frac{2\pi}{r} \left(\frac{\epsilon}{\bar{\xi}} + \delta \right). \quad (75)$$

To estimate v , we assume that it takes a value in between its value for a classical matter-dominated universe at time t_j , and a de Sitter universe, for which $v = 0$. In a classical matter-dominated universe, v is given by Eq.(58) as

$$v = -\frac{\rho_m^2}{960m^4\kappa_o^2}. \quad (76)$$

At time t_j , $\rho_m = \rho_{mj} = 2\kappa_o\bar{m}^2$. Therefore, at t_j , we obtain

$$v_j = -(240\bar{\xi}^2)^{-1}. \quad (77)$$

We therefore assume that, for $t > t_j$, v lies in the range

$$-(240\bar{\xi}^2)^{-1} < v < 0. \quad (78)$$

It is convenient to define an additional quantity

$$\beta = \frac{r}{2\pi} \left(v - \frac{1}{2(1080)\bar{\xi}^2} \right). \quad (79)$$

For $r \ll 1$, and v given by Eq. (78), it follows that $|\beta| \ll 1$. One may now solve Eq. (75) for ϵ . This yields

$$\epsilon = -\frac{1}{2}\bar{\xi} \left(\delta \pm \left(\delta^2 + 4\beta\bar{\xi}^{-1} \right) \right). \quad (80)$$

In order to choose the correct sign in the above equation, we will require that the scalar curvature approach its classical value $\rho_m/(2\kappa_o)$ for large values of the matter density, i.e. for $\rho_m/(2m^2\kappa_o) \gg 1$. For large matter densities, δ is a large negative number. To get the correct value of the scalar curvature, one must then choose the solution with the minus sign in the above equation. Even though this value of ϵ is not small, continuity demands that we keep the solution with the same sign for all δ . Thus we have

$$\epsilon = -\frac{1}{2}\bar{\xi} \left(\delta - \left(\delta^2 - 4\beta\bar{\xi}^{-1} \right) \right). \quad (81)$$

It is clear, for $\delta > 0$, that $|\epsilon|$ is always a small number, reaching a maximum value of $\sqrt{\beta\bar{\xi}}$ at $\delta = 0$ (we have assumed that $r \ll 1$).

The approximation $|\epsilon| \ll 1$, which was made in order to arrive at the solution (81), is thus valid for $t \geq t_j$. Within this range of time, the value of ϵ evolves from

$$\epsilon(t_j) = \sqrt{\beta\bar{\xi}} \quad (82)$$

when $\rho_m = \rho_{mj}$ ($\delta = 0$), to

$$\epsilon(\infty) \simeq -\beta\bar{\xi} \quad (83)$$

when $\rho_m = 0$ ($\delta = -\bar{\xi}^{-1}$). The fractional change in the scalar curvature during this range of time is given by Eq. (72) as

$$\frac{\Delta R}{R} = \frac{-\bar{m}^2 \Delta \epsilon}{\bar{m}^2(1-\epsilon)} \simeq -\Delta \epsilon, \quad (84)$$

because $|\epsilon| \ll 1$ during the entire time range. Thus, with $\Delta \epsilon = \epsilon(\infty) - \epsilon(t_j)$, we obtain

$$\left| \frac{\Delta R}{R} \right| \simeq \sqrt{\beta \bar{\xi}} \left(1 + \sqrt{\beta \bar{\xi}} \right) \ll 1, \quad (85)$$

because $r \ll 1$.

To summarize, we have argued that, even in the presence of matter, there exist de Sitter type solutions in which the scalar curvature is very close to the value \bar{m}^2 , and is very slowly varying, as long as the matter density is such that $\delta \geq 0$. For large negative values of δ , i.e. large ρ_m in Eq. (74), it is clear that the scalar curvature continuously changes to the scalar curvature of a matter-dominated universe.

Coupled with the findings of the previous subsection, in which we showed that quantum effects near t_j tend to prevent the scalar curvature from decreasing further, these results strongly point to a cosmology in which a matter-dominated universe transits to a de Sitter-type universe. In the next subsection, we outline such a model.

VII. MATTER DOMINATED EXPANSION LEADING INTO ACCELERATED EXPANSION

The damping of scalar curvature, which begins at a time close to t_j , supports the idea that the universe undergoes a transition from a matter-dominated phase to a mildly inflationary de Sitter phase. The arguments of the previous subsection show that the de Sitter phase is, to good approximation, described by a solution with $\bar{\xi} < 0$ and $R \simeq \bar{m}^2$, of the type found in the Section V, and that the presence of matter does not significantly change such a solution. Within a rigorous framework, the matter-dominated and de Sitter phases must be joined in a sufficiently smooth manner to guarantee regularity of all curvature components at the joining point. However, the perturbative analysis of the previous subsection shows that the quantum effects become significant over a short timescale, after which the scalar curvature approaches a constant value. This effect allows us to consider, for comparison with observation, an approximation in which an exact classical matter-dominated solution is joined (at time t_j) to a de Sitter solution generated by quantum effects. Assuming a spatially open cosmology ($k = -1$ in Eq. (59)), such a model is represented by the following scale factor:

$$\begin{aligned} a(t) &= c_0 \sinh^2(\psi/2), & t &= \frac{1}{2}c_0(\sinh \psi - \psi), & t < t_j \\ a(t) &= \alpha^{-1} \sinh(\alpha(t + c_1)), & t &> t_j. \end{aligned} \quad (86)$$

Here, ψ parametrizes $a(t)$ and t during the matter-dominated stage. For $t > t_j$, including the present time t_0 , the universe is in a de Sitter phase.

Of the five parameters, c_0 , α , t_j , c_1 and the present cosmic time t_0 , that characterize the model based on Eq. (86), not all are independent. The scalar curvature at the time of joining, R_j , must be equal to the constant scalar curvature during the later, inflationary phase, and is determined by the *single* scale $\bar{m} \equiv m/\sqrt{-\bar{\xi}}$. This requirement and the requirement of continuity of the scale factor at the joining point, constitute two constraints on the five parameters. The remaining three parameters can, for convenience, be taken to be (i) the present Hubble constant H_0 , (ii) the present ratio of matter density to critical density Ω_0 , and (iii) the mass scale \bar{m} . Here, we express the five parameters defining the model of Eq. (86) in terms of these three basic parameters.

First, the scalar curvature during the later, de Sitter phase is given by $12\alpha^2$. Setting this equal to \bar{m}^2 , as required by the de Sitter solutions of Section V, we get the relation

$$\alpha = \frac{\bar{m}}{\sqrt{12}}. \quad (87)$$

The scalar curvature during the matter-dominated phase is given by $R = 3c_0a^{-3}$. The classical Einstein equations, which hold during the matter-dominated phase, thus imply

$$3c_0 = (8\pi G)\rho_{mj}a_j^3 = (8\pi G)\rho_{m0}a_0^3, \quad (88)$$

where a_j and a_0 represent the scale factor at t_j and the present time t_0 , respectively, and ρ_{mj} and ρ_{m0} are the corresponding matter densities. The second equality in the above equation follows from the fact that $\rho_m a^3$ is constant during the evolution, a consequence of conservation of the matter stress-energy.

Thus, Eq. (88) gives

$$c_0/a_0^3 = \Omega_0 H_0^2, \quad (89)$$

where $\Omega_0 = 8\pi G\rho_{m0}/(3H_0^2)$ is the present ratio of matter density to critical density.

The Hubble constant at the present time is given by Eq. (86) as

$$\begin{aligned} H_0 &= \alpha \coth(\alpha(t_0 + c_1)) \\ &= a_0^{-1} \sqrt{1 + a_0^2 \alpha^2}, \end{aligned} \quad (90)$$

where a_0 is the scale factor at the present time t_0 . We solve for a_0 , and use Eq. (87) to get

$$a_0 = (H_0^2 - \bar{m}^2/12)^{-1/2}. \quad (91)$$

Combining Eqs. (89) and (91), we obtain

$$c_0 = \Omega_0 H_0^2 (H_0^2 - \bar{m}^2/12)^{-3/2}. \quad (92)$$

We may obtain the scale factor at time t_j , a_j , by requiring that the scalar curvature of the matter-dominated phase approach the value \bar{m}^2 as $t \rightarrow t_j^-$. This condition yields

$$a_j^3 = \frac{3c_0}{\bar{m}^2}. \quad (93)$$

Substituting for c_0 from Eq. (92), we then have

$$a_j = (3\Omega_0 H_0^2 / \bar{m}^2)^{1/3} (H_0^2 - \bar{m}^2/12)^{-1/2}. \quad (94)$$

To obtain t_j , we use the matter-dominated solution in Eq. (86) to get

$$\psi_j = 2 \sinh^{-1} \sqrt{a_j c_0^{-1}} \quad (95)$$

and

$$\begin{aligned} t_j &= \frac{1}{2} c_0 (\sinh \psi_j - \psi_j) \\ &= c_0 \left(\sqrt{(a_j c_0^{-1})(1 + a_j c_0^{-1})} - \sinh^{-1} \sqrt{a_j c_0^{-1}} \right). \end{aligned} \quad (96)$$

To obtain c_1 , we use the de Sitter solution in Eq. (86) to get

$$c_1 = \alpha^{-1} \sinh^{-1}(\alpha a_j) - t_j. \quad (97)$$

Finally, to obtain the present cosmic time t_0 , we again use the de Sitter solution, which yields

$$t_0 = \alpha^{-1} (\sinh^{-1}(\alpha a_0) - \sinh^{-1}(\alpha a_j)) + t_j. \quad (98)$$

All parameters in the model are now expressed in terms of \bar{m} , H_0 and Ω_0 .

In the next section, we will compare the predictions of this model to recent data from high-redshift Type 1a supernovae [6], using magnitude-redshift curves obtained from our model.

VIII. COMPARISON OF THEORY WITH HIGH-Z SUPERNOVAE DATA; PREDICTION OF PARTICLE WITH MASS $\sim 10^{-33}$ EV

Recent observations of Type 1a supernovae at high redshifts indicate a negative value of the deceleration parameter at the present time, i.e. an accelerating universe [6]. Previous attempts to account for this phenomenon invoke a cosmological constant, or a classical scalar field, quintessence [23], with unusual potentials. To explain the observed acceleration effect by means of a cosmological constant, it must contribute a term to the Einstein equations that is of the same order of magnitude as that attributed by the present matter density. On the other hand, quintessence

models that account for the acceleration effect typically involve potentials that would give rise to nonrenormalizable quantum field theories.

In the model we present here, the value of H_0 is fixed by low-redshift measurements, while the remaining free parameters \bar{m} and Ω_0 are determined by the SNe-Ia data. Once the mass scale \bar{m} is determined, no fundamental parameters in the effective action need be chosen to fit the supernovae data. Furthermore, the theory we work with arises out of a renormalized effective action.

Comparison of our model to SNe-Ia data is achieved by fitting calculated magnitude-redshift curves to the data. The difference between the apparent magnitude (m) and absolute magnitude (M) of a source is given in terms of the luminosity distance d_L to the source, by

$$m - M = 5 \log_{10} \frac{d_L}{\text{Mpc}} + 25. \quad (99)$$

The luminosity distance itself is given by [24]

$$d_L = (1 + z)a_0 r_1, \quad (100)$$

where a_0 is the present scale factor, and r_1 is the comoving coordinate distance from a source at redshift z to a detector at redshift 0. For Robertson-Walker universes, r_1 is given by the equation

$$\int_0^{r_1} \frac{dr}{(1 - kr^2)^{\frac{1}{2}}} = a_0^{-1} \int_0^z \frac{dz'}{H(z')}, \quad (101)$$

where $k = 0, +1, -1$ correspond to flat, closed and open universes, respectively. For a spatially open universe, the above equation reduces to

$$\sinh^{-1} r_1 = a_0^{-1} \int_0^z \frac{dz'}{H(z')}. \quad (102)$$

Consider a universe represented by the model of Eq. (86), which is a spatially open matter-dominated universe prior to time t_j , and transits into a de Sitter universe at t_j . Let z_j be the redshift at time t_j . For $z < z_j$, the universe is in a de Sitter phase, with Hubble constant given by

$$\begin{aligned} H &= \alpha \coth \alpha(t + c_1) \\ &= \sqrt{\alpha^2 + \frac{(1+z)^2}{a_0^2}}. \end{aligned} \quad (103)$$

Substituting the above into Eq. (102), and performing the integration, we obtain, for $z < z_j$,

$$r_{1<}(z) = \frac{1+z}{(a_0\alpha)^2} \left(\sqrt{1 + (a_0\alpha)^2} - \sqrt{1 + \left(\frac{a_0\alpha}{1+z}\right)^2} \right), \quad (104)$$

where $r_{1<}(z)$ denotes $r_1(z)$ for $z < z_j$. For $z > z_j$, the RHS of Eq. (102) separates into two contributions:

$$\sinh^{-1}(r_{1>}) = a_0^{-1} \left(\int_0^{z_j} \frac{dz'}{H(z')} + \int_{z_j}^z \frac{dz'}{H(z')} \right), \quad (105)$$

where $r_{1>}(z)$ denotes $r_1(z)$ for $z > z_j$.

During the matter-dominated phase, the Hubble constant is calculated as

$$\begin{aligned} H &= \sqrt{c_0 a^{-3} + a^{-2}} \\ &= \frac{1+z}{a_0} \sqrt{1 + c_0 a_0^{-1} (1+z)}. \end{aligned} \quad (106)$$

Using Eq. (103) for $z' < z_j$ and Eq. (106) for $z' > z_j$, the integrations in Eq. (105) may be performed to yield

$$r_{1>}(z) = \sinh \left(\sinh^{-1}(r_{1<}(z_j)) + \ln \left(\frac{(g(z) - 1)(g(z_j) + 1)}{(g(z) + 1)(g(z_j) - 1)} \right) \right), \quad (107)$$

where

$$g(z) = \sqrt{1 + c_0 a_0^{-1} (1 + z)}. \quad (108)$$

Eq. (100) gives the luminosity distance, d_{L1} , for this model, as

$$\begin{aligned} d_{L1} &= (1 + z) a_0 r_{1<}(z), \quad z < z_j \\ &= (1 + z) a_0 r_{1>}(z), \quad z > z_j. \end{aligned} \quad (109)$$

For comparison, the luminosity-distance-redshift relation for a matter-dominated Robertson-Walker universe with zero cosmological constant and ratio Ω_0 of present matter density to critical density, is

$$d_{L2}(\Omega_0, z) = 2H_0^{-1} \Omega_0^{-2} \left(\Omega_0 z + (\Omega_0 - 2)(\sqrt{1 + \Omega_0 z} - 1) \right), \quad (110)$$

and for a spatially flat matter-dominated ($\Omega_0 = 1$) universe,

$$d_{L2}(1, z) = 2H_0^{-1} \sqrt{1 + z} (\sqrt{1 + z} - 1). \quad (111)$$

It is convenient (see Eq. (99)) to define

$$\Delta(m - M)(z) = 5 \log_{10} \left(\frac{d_L(z)}{d_{L2}(0.2, z)} \right). \quad (112)$$

Fig. 3 is a plot of $\Delta(m - M)$ vs. z , along with a plot of SNe-Ia data acquired from Ref. [6]. The two solid curves represent $d_L(z) = d_{L1}(z)$. In plotting this quantity, all parameters appearing in d_{L1} have been expressed in terms of the three basic parameters \overline{m} , H_0 and Ω_0 , using the relations derived in the previous section. Also, the value of H_0 has been set to 65 km/(s Mpc). Thus there are two quantities, \overline{m} and Ω_0 , which parametrize the solid curves. The two curves shown in the figure give a reasonable fit to the data, and correspond to a) $\overline{m} = 3.7 \times 10^{-33}$ eV and $\Omega_0 = 0.4$ (higher solid curve), and b) $\overline{m} = 3.2 \times 10^{-33}$ eV and $\Omega_0 = 0.3$ (lower solid curve).

The general features of a family of curves parametrized by (\overline{m}, Ω_0) are as follows. For a fixed value of \overline{m} , decreasing Ω_0 has the sole effect of increasing the redshift at which the transition occurs, i.e. a smaller value of Ω_0 will move the transition further from the present time. Thus we cannot rule out the possibility that, with more observations at higher redshift, a better fit to the data could be obtained with lower values of Ω_0 . However, the data do not allow the joining points in Fig. (3) to occur at smaller z_j , so the values of Ω_0 shown in the plot do represent a rough upper bound on Ω_0 in our model, and lead to the conclusion stated earlier, $\Omega_0 < 0.4$. As is well known, an *early* inflationary epoch would explain why Ω_0 is not very far from 1.

For a fixed value of Ω_0 , increasing \overline{m} has the effect of shifting the curves up, as well as increasing somewhat the redshift at which the transition occurs.

The two dashed curves in Fig. (3) are shown for comparison, and represent c) $d_L = d_{L2}(0.2, z)$ (horizontal dashed line), i.e. an open matter-dominated universe with $\Omega_m = 0.2$, and d) $d_L = d_{L2}(1, z)$ (lower dashed curve), i.e. a spatially flat matter-dominated universe.

IX. THE AGE OF THE UNIVERSE

As stated earlier, the only fundamental scale that enters into the effective action of the model presented here is \overline{m} . Nevertheless, as we show now, the fit of our model to supernovae data predicts reasonable values for the age of the universe t_0 .

The relations derived in Section VII, leading up to Eqs. (96) and (98), give t_j and t_0 in terms of \overline{m} , Ω_0 and H_0 . For $H_0 = 65$ km/(s Mpc), $\overline{m} = 3.7 \times 10^{-33}$ eV, and $\Omega_0 = 0.4$ (upper solid curve in Fig. 3), we obtain

$$t_j = 5.66 \times 10^9 \text{ years} \quad (113)$$

$$t_0 = 1.34 \times 10^{10} \text{ years}. \quad (114)$$

For $H_0 = 65$ km/(s Mpc), $\overline{m} = 3.2 \times 10^{-33}$ eV and $\Omega_0 = 0.3$, we obtain

$$t_j = 6.03 \times 10^9 \text{ years} \quad (115)$$

$$t_0 = 1.33 \times 10^{10} \text{ years}. \quad (116)$$

Therefore, in both cases a reasonable value of roughly 13 billion years is obtained for the age of the universe. More data at higher redshifts may lower the value of Ω_0 in our model, which would further increase the age of the universe.

Fig. 4 contains plots of the scale factor versus cosmic time for the two solid curves of Fig. 3. In each case, the open matter-dominated universe that transits to the de Sitter phase is shown continued as a dashed curve, for comparison.

X. CONCLUSIONS

In summary, we showed that a model in which a transition occurs from a matter-dominated to a de Sitter expansion, fits the SNe-Ia data. We call such a model, a transitional universe. Also, we have proposed a free quantum field theory effective action, Eq. (38), in which such a transition evidently occurs. The existence of a particle of very low mass would cause the universe to make a transition from the matter-dominated to a new de Sitter stage. In our model, one can say that we are now observing the mass scale of this particle through the SNe-Ia data.

Models involving interacting fields may also give a transitional universe, and such models would be natural extensions of the free field model presented here as the simplest case.

We emphasize once again that the solutions to the gravitational field equations we obtain, in particular the de Sitter solutions for $\bar{\xi} < 0$, exist without the necessity of a non-zero cosmological constant term in the effective action. Furthermore, these solutions are fairly insensitive to the presence of a cosmological constant term. In this manner, our model does not suffer from the problem of fine-tuning of the cosmological constant, which exists in mixed matter and vacuum energy models.

The present matter density and the predicted age of the universe agree well with the current estimates. As in other models, a value of Ω_0 not far from 1 may result from a period of early inflation. Further constraints on Ω_0 and \bar{m} in our model could result from comparison to cosmic microwave background data, as well as from the time-temperature relationship during nucleosynthesis. We hope to carry out such a comparison in the future.

Finally, we would like to mention that the R -summed form of the effective action could have consequences for early universe cosmology as well. In particular, the existence of an imaginary term in the effective action, implying particle creation effects, could play a role in the exit from an inflationary universe. In future work, we plan to pursue these ideas as well as to carry out a dynamical calculation giving the details of the transition between the matter-dominated stage and the later de Sitter stage of the expansion.

Acknowledgements

This work was supported by NSF grant PHY-9507740.

APPENDIX A: DIVERGENCES IN THE EFFECTIVE ACTION AS $M^2 \rightarrow 0^+$

Consider the one-loop effective action in Eq. (30) below threshold, i.e. $M^2 > 0$. This action is then a real series which is divergent as $M^2 \rightarrow 0$. The part of the first term in this series, involving M^4 , vanishes in this limit. However, subsequent terms, involving \bar{f}_l for $l \geq 2$, are all divergent as $M^2 \rightarrow 0$. All terms containing \bar{f}_3 and higher orders correspond to an asymptotic series in inverse powers of M^2 and therefore do not give a valid expansion for small values of M^2 . The behavior of this expansion as $M^2 \rightarrow 0$ is thus unphysical and does not seem to be a cause for concern⁸. However, the term $\bar{f}_2 \ln(M^2)$ is also divergent in this limit and is physically required for renormalization of ultraviolet (UV) divergences and to obtain the trace anomaly. It is therefore of interest to examine in detail the divergent behavior of this term as $M^2 \rightarrow 0$. We will show here that this divergence, although infrared in nature, can be absorbed into the ultraviolet divergences of the theory by a procedure similar to the way infrared divergences at $m = 0$ are handled in the usual one-loop effective action [12]. To this end, we will consider the one-loop effective action (30), truncated up to the terms involving \bar{f}_2 . We will work within the dimensional regularization scheme, which is more useful than the zeta function scheme in this context because the divergent terms are explicitly displayed.

First, Eq. (4) implies the following proper time representation of the effective action [10,12]:

$$\begin{aligned} W^1 &= -\frac{i}{2} \text{Tr} \int_0^\infty ds s^{-1} e^{-isH} \\ &= \frac{1}{2} (\mu^2)^{2-D/2} \int d^D x \sqrt{-g} \int_0^\infty ds (is)^{-1} (4\pi is)^{-D/2} e^{-is(M^2 - i\epsilon)} \bar{F}(x, x, is). \end{aligned} \quad (\text{A1})$$

The truncated one-loop effective action before renormalization is obtained, in four dimensions, by keeping the first three terms in a power series expansion of \bar{F} in Eq. (15). These terms include UV-divergent contributions to the effective action arising from the behavior of the integrand near $s = 0$. All higher order terms are UV-finite.

Thus we obtain for the truncated one-loop effective action

$$W_{\text{trun}}^1 = \frac{1}{2} (4\pi)^{-D/2} (\mu^2)^{2-D/2} \int d^D x \sqrt{-g} \int_0^\infty ds (is)^{-D/2-1} e^{-is(M^2 - i\epsilon)} (1 + (is)^2 \bar{f}_2), \quad (\text{A2})$$

where we have set $\bar{f}_1 = 0$ without loss of generality. The above equation has a finite piece corresponding to the sum over all powers of s higher than 2 in the expansion of $e^{-is\bar{\xi}R}$ in the integrand. Therefore W_{trun}^1 as defined above differs from what is usually regarded as the divergent part of the effective action by this finite piece. Here, we need to keep this extra piece in order to properly take the limit $M^2 \rightarrow 0$.

In performing dimensional regularization about $D = 4$, it is convenient to define $2\delta = D - 4$. One can perform the proper time integral in Eq. (A2), to get

$$W_{\text{trun}}^1 = (32\pi^2)^{-1} \int d^4 x \sqrt{-g} \left\{ \mu^4 \left(\frac{M^2}{\mu^2} \right)^{2+\delta} \Gamma(-2-\delta) + \bar{f}_2 \left(\frac{M^2}{\mu^2} \right)^\delta \Gamma(-\delta) \right\}. \quad (\text{A3})$$

Expanding the exponents and the Gamma functions about $\delta = 0$ ($D = 4$), we get

$$\begin{aligned} W_{\text{trun}}^1 &= (32\pi^2)^{-1} \int d^4 x \sqrt{-g} \left\{ M^4 \left(\frac{1}{4-D} - \frac{\gamma}{2} + \frac{3}{4} - \frac{1}{2} \ln(M^2/\mu^2) \right) \right. \\ &\quad \left. + \bar{f}_2 \left(\frac{2}{4-D} - \gamma - \ln(M^2/\mu^2) \right) \right\} + \mathcal{O}(D-4). \end{aligned} \quad (\text{A4})$$

The expression above already indicates that the divergence as $M^2 \rightarrow 0$ may be absorbed into the UV-divergence as $D \rightarrow 4$ in the coefficient of \bar{f}_2 . To see this explicitly, we may set $M^2 = 0$ in Eq. (A2) at the outset, and replace the upper limit of the s -integration by some large number T to regularize the integral (infrared regularization). We can then examine the divergent behavior as $T \rightarrow \infty$. We therefore have

⁸It is possible that all higher order terms sum to give a finite contribution as $M^2 \rightarrow 0$. An example of such a situation is the series $(1-x^{-1})^{-1} = \sum_{n=0}^\infty x^{-n}$, which is a valid expansion for $x > 1$. As $x \rightarrow 0$, every term on the right hand side is divergent, although the left hand side vanishes.

$$W_{\text{trun}}^1 = (32\pi^2)^{-1}(\mu^2)^{2-D/2} \int d^D x \sqrt{-g} \int_0^T ds (is)^{-D/2-1} e^{-s\epsilon} (1 + (is)^2 \bar{f}_2), \quad (\text{A5})$$

which may be evaluated in terms of the incomplete Gamma functions $\gamma(\alpha, x)$,

$$W_{\text{trun}}^1 = (32\pi^2)^{-1} \int d^4 x \sqrt{-g} \left\{ i^{-D/2} (\epsilon/\mu^2)^{D/2} \gamma(-D/2, \epsilon T) + i^{-D/2+2} \bar{f}_2 (\epsilon/\mu^2)^{D/2-2} \gamma(2-D/2, \epsilon T) \right\}. \quad (\text{A6})$$

We may now take the limit $\epsilon \rightarrow 0$ of the above expression by using the power series expansion [25]

$$\gamma(\alpha, x) = \sum_{n=0}^{\infty} \frac{(-1)^n x^{\alpha+n}}{n!(\alpha+n)}. \quad (\text{A7})$$

This yields, after some simplification

$$W_{\text{trun}}^1 = (32\pi^2)^{-1} \int d^4 x \sqrt{-g} \left\{ \frac{1}{2} T^{-2} + \bar{f}_2 \left(\frac{2}{4-D} + \ln(\mu^2 T) \right) + \mathcal{O}(D-4) \right\}. \quad (\text{A8})$$

As $T \rightarrow \infty$, the first term in Eq. (A8) drops out, leaving behind a term proportional to \bar{f}_2 which diverges logarithmically in this limit. However, this divergence can be absorbed into the UV-divergence as $D \rightarrow 4$.

We therefore find that the logarithmic divergence in the effective action in the ‘‘infrared’’ limit $T \rightarrow \infty$ may be canceled by counterterms of the same geometric form as the ones introduced into the bare gravitational action to cancel the UV divergences as $D \rightarrow 4$, i.e. a counterterm proportional to \bar{f}_2 is required here. The infrared problem in the partially summed form of the effective action is thus handled in a way similar to the infrared divergence in the usual effective action at $m = 0$, where a counterterm proportional to f_2 is required.

The analysis above may be carried out in a similar manner even when we do not set $M^2 = 0$ at the very beginning but rather let M^2 tend to zero from positive values. Eq. (A8) is recovered at the end of the calculation.

APPENDIX B: VARIATIONS OF CURVATURE INVARIANTS

Here we will list the variations of the curvature invariants that occur in the effective action in Eq. (38). They are as follows:

$$\delta \left(\int d^4 x \sqrt{-g} R \right) = - \int d^4 x \sqrt{-g} \delta g_{\mu\nu} G^{\mu\nu} \quad (\text{B1})$$

$$\delta \left(\int d^4 x \sqrt{-g} R^2 \right) = \int d^4 x \sqrt{-g} \delta g_{\mu\nu} \left\{ \frac{1}{2} g^{\mu\nu} R^2 - 2RR^{\mu\nu} + 2R^{:\nu\mu} - 2g^{\mu\nu} \square R \right\} \quad (\text{B2})$$

$$\begin{aligned} \delta \left(\int d^4 x \sqrt{-g} \ln | M^2/m^2 | \right) &= \int d^4 x \sqrt{-g} \delta g_{\mu\nu} \left\{ -\bar{\xi} M^{-2} R^{\mu\nu} - \bar{\xi} g^{\mu\nu} \left(2M^{-6} \bar{\xi}^2 R_{;\alpha} R^{;\alpha} \right. \right. \\ &\left. \left. - M^{-4} \bar{\xi} \square R \right) + \bar{\xi} \left(2M^{-6} R^{;\mu} R^{;\nu} - M^{-4} \bar{\xi} R^{;\nu\mu} \right) + \frac{1}{2} g^{\mu\nu} \ln | M^2/m^2 | \right\} \end{aligned} \quad (\text{B3})$$

$$\begin{aligned} \delta \left(\int d^4 x \sqrt{-g} R \ln | M^2/m^2 | \right) &= \int d^4 x \sqrt{-g} \delta g_{\mu\nu} \left\{ -G^{\mu\nu} \ln | M^2/m^2 | - \bar{\xi} M^{-2} R R^{\mu\nu} \right. \\ &\left. + \bar{\xi} \frac{m^2 + M^2}{M^4} (R^{;\mu\nu} - g^{\mu\nu} \square R) - \bar{\xi}^2 \frac{2m^2 + M^2}{M^6} (R^{;\mu} R^{;\nu} - g^{\mu\nu} R_{;\alpha} R^{;\alpha}) \right\} \end{aligned} \quad (\text{B4})$$

$$\begin{aligned} \delta \left(\int d^4 x \sqrt{-g} R^2 \ln | M^2/m^2 | \right) &= \int d^4 x \sqrt{-g} \delta g_{\mu\nu} \left\{ \ln | M^2/m^2 | \left(\frac{1}{2} g^{\mu\nu} R^2 - 2RR^{\mu\nu} \right. \right. \\ &\left. \left. + 2R^{;\nu\mu} \right) + \bar{\xi} M^{-2} \left(-R^2 R^{\mu\nu} + 6R^{;\mu} R^{;\nu} + 4RR^{;\nu\mu} \right) - \bar{\xi}^2 M^{-4} R \left(6R^{;\mu} R^{;\nu} \right. \right. \\ &\left. \left. + RR^{;\nu\mu} \right) + 2\bar{\xi}^3 M^{-6} R^2 R^{;\mu} R^{;\nu} \right\} \end{aligned} \quad (\text{B5})$$

$$\begin{aligned} \delta\left(\int d^4x\sqrt{-g}\bar{f}_2\right) &= \frac{1}{180}\int d^4x\sqrt{-g}\delta g_{\mu\nu}\left\{3\Box R^{\mu\nu}-R^{;\mu\nu}-\frac{1}{2}g^{\mu\nu}\Box R\right. \\ &\left.+2R^{\mu\sigma\nu\tau}R_{\sigma\tau}+\frac{1}{2}g^{\mu\nu}R_{\sigma\tau}R^{\sigma\tau}+2R^\mu{}_{\sigma\tau\rho}R^{\nu\sigma\tau\rho}-\frac{1}{2}g^{\mu\nu}R_{\sigma\tau\rho\lambda}R^{\sigma\tau\rho\lambda}-4R^\mu{}_\sigma R^{\nu\sigma}\right\} \end{aligned} \quad (\text{B6})$$

$$\begin{aligned} \delta\left(\int d^4x\sqrt{-g}\Box R\ln|M^2/m^2|\right) &= \int d^4x\sqrt{-g}\delta g_{\mu\nu}\bar{\xi}M^{-2}\left\{-2g^{\mu\nu}\Box\Box R+2(\Box R)^{;\mu\nu}\right. \\ &-\frac{1}{2}g^{\mu\nu}R^{;\alpha}R_{;\alpha}+R^{;\mu}R_{;\nu}+\bar{\xi}M^{-2}\left(4g^{\mu\nu}(\Box R)^{;\alpha}R_{;\alpha}+2g^{\mu\nu}(\Box R)^2-4R^{;(\mu}(\Box R)^{;\nu)}-2\Box R R^{;\mu\nu}\right. \\ &+R^{\mu\nu}R^{;\alpha}R_{;\alpha}+2R^{;\alpha}(g^{\mu\nu}\Box-\nabla^\mu\nabla^\nu)R_{;\alpha}+2g^{\mu\nu}R_{;\alpha\beta}R^{;\alpha\beta}-2R_{;\alpha}{}^\nu R^{;\alpha\mu}) \\ &+2\bar{\xi}^2M^{-4}\left(-R_{;\alpha}R^{;\alpha}(g^{\mu\nu}\Box-\nabla^\mu\nabla^\nu)R+4R^{;(\mu}R_{\alpha}{}^{\nu)}R^{;\alpha}-4g^{\mu\nu}R^{;\alpha}R^{;\beta}R_{;\alpha\beta}\right) \\ &\left.+6\bar{\xi}^3M^{-6}(g^{\mu\nu}R_{;\alpha}R^{;\alpha}-R^{;\mu}R^{;\nu})\right\} \end{aligned} \quad (\text{B7})$$

$$\begin{aligned} \delta\left(\int d^4x\sqrt{-g}R^{\alpha\beta}R_{\alpha\beta}\ln|M^2/m^2|\right) &= \int d^4x\sqrt{-g}\delta g_{\mu\nu}\left\{\ln|M^2/m^2|\left(\frac{1}{2}g^{\mu\nu}R^{\alpha\beta}R_{\alpha\beta}-3R^{\mu\alpha}R_{\alpha}{}^\nu\right.\right. \\ &+ \left.\Box R^{\mu\nu}+\frac{1}{2}g^{\mu\nu}\Box R-R^{;\mu\nu}+R^{\alpha\nu\beta\mu}R_{\alpha\beta}\right)+\bar{\xi}M^{-2}\left(-R^{\mu\nu}R^{\alpha\beta}R_{\alpha\beta}+R^{\mu\nu}\Box R-2R^{\alpha(\mu}R_{;\alpha}{}^{\nu)}\right. \\ &+g^{\mu\nu}R^{\alpha\beta}R_{;\alpha\beta}+2R_{;\alpha}R^{\mu\nu;\alpha}+g^{\mu\nu}R_{;\alpha}R^{;\alpha}-R^{;\mu}R^{;\nu}-2R_{;\alpha}R^{\alpha(\mu;\nu)}-2g^{\mu\nu}R^{\alpha\beta}\Box R_{\alpha\beta} \\ &-2g^{\mu\nu}R_{\alpha\beta;\kappa}R^{\alpha\beta}{}_{;\kappa}+2R_{\alpha\beta}{}^{;\nu\mu}R^{\alpha\beta}+2R_{\alpha\beta}{}^{;\mu}R^{\alpha\beta;\nu})+\bar{\xi}^2M^{-4}\left(-R^{\mu\nu}R_{;\alpha}R^{;\alpha}-g^{\mu\nu}R^{\alpha\beta}R_{;\alpha}R_{;\beta}\right. \\ &+2R^{;(\mu}R^{\nu)\alpha}R_{;\alpha}+4g^{\mu\nu}R^{\alpha\beta}R_{;\kappa}R_{\alpha\beta;\kappa}+g^{\mu\nu}R_{\alpha\beta}R^{\alpha\beta}\Box R-4R_{\alpha\beta}{}^{;(\mu}R^{;\nu)}R^{\alpha\beta}-R^{\alpha\beta}R_{\alpha\beta}R^{;\mu\nu}) \\ &\left.+2\bar{\xi}^3M^{-6}R^{\alpha\beta}R_{\alpha\beta}(R^{;\mu}R^{;\nu}-g^{\mu\nu}R_{;\alpha}R^{;\alpha})\right\} \end{aligned} \quad (\text{B8})$$

$$\begin{aligned} \delta\left(\int d^4x\sqrt{-g}R^{\alpha\beta\gamma\delta}R_{\alpha\beta\gamma\delta}\ln|M^2/m^2|\right) &= \int d^4x\sqrt{-g}\delta g_{\mu\nu}\left\{\ln|M^2/m^2|\left(\frac{1}{2}g^{\mu\nu}R^{\alpha\beta\gamma\delta}R_{\alpha\beta\gamma\delta}\right.\right. \\ &-2R^{\mu\kappa\gamma\delta}R^\nu{}_{\kappa\gamma\delta}-4R^{\beta\nu\alpha\mu}{}_{;\beta\alpha}+\bar{\xi}M^{-2}\left(-R^{\mu\nu}R^{\alpha\beta\gamma\delta}R_{\alpha\beta\gamma\delta}-2g^{\mu\nu}R^{\alpha\beta\gamma\delta}R_{\alpha\beta\gamma\delta;\kappa}{}^\kappa\right. \\ &-2g^{\mu\nu}R^{\alpha\beta\gamma\delta;\kappa}R_{\alpha\beta\gamma\delta;\kappa}+2R_{\alpha\beta\gamma\delta}{}^{;\nu\mu}R^{\alpha\beta\gamma\delta}+2R_{\alpha\beta\gamma\delta}{}^{;\nu}R^{\alpha\beta\gamma\delta;\mu}-4R^{\beta\nu\alpha\mu}{}_{;\alpha}R_{;\beta}-4R^{\beta\nu\alpha\mu}R_{;\beta\alpha}) \\ &+ \left.\bar{\xi}^2M^{-4}\left(4g^{\mu\nu}R^{\alpha\beta\gamma\delta}R_{\alpha\beta\gamma\delta}{}^{;\kappa}R_{;\kappa}+g^{\mu\nu}R^{\alpha\beta\gamma\delta}R_{\alpha\beta\gamma\delta}\Box R-4R^{\alpha\beta\gamma\delta}R_{\alpha\beta\gamma\delta}{}^{;(\nu}R^{;\mu)}-R^{\alpha\beta\gamma\delta}R_{\alpha\beta\gamma\delta}R^{;\mu\nu}\right.\right. \\ &\left.\left.+4R^{\beta\nu\alpha\mu}R_{;\beta}R_{;\alpha}\right)+2\bar{\xi}^3M^{-6}\left(-g^{\mu\nu}R_{;\alpha}R^{;\alpha}+R^{;\mu}R^{;\nu}\right)\right\} \end{aligned} \quad (\text{B9})$$

-
- [1] L. Parker, Ph.D. thesis, Harvard University, 1966 (available from Xerox University microfilms); Phys. Rev. Lett. **21**, 562 (1968); Phys. Rev. **183**, 1057 (1969).
- [2] S. W. Hawking, Commun. Math. Phys. **43**, 199 (1975).
- [3] L. Parker and D. J. Toms, Phys. Rev. D **31**, 953 (1985); Phys. Rev. D **31**, 2424 (1985).
- [4] E. Elizalde, C. O. Lousto, S. D. Odintsov and A. Romeo, Phys. Rev. D **52**, 2202 (1995); J. Barrow and A. Ottewill, J. Phys. A **16**, 2757 (1983); J. Barrow, Phys. Lett. B **183**, 285 (1987), Nucl. Phys. **B296**, 697 (1988); M. Mijic, M. Morris, and W.-M. Suen, Phys. Rev. D **34**, 2934 (1986); A. Starobinsky and H. J. Schmidt, Class. Quantum Grav. **4**, 695 (1987); M. Campanelli, C. O. Lousto and J. Audretsch, Phys. Rev. D **49**, 5188 (1994); R. Brandenberger, V. Mukhanov, and A. Sornberger, Phys. Rev. D **48**, 1629 (1993).
- [5] S. Perlmutter *et al.*, *Nature* 391, 51 (1998).
- [6] A. G. Reiss *et al.*, astro-ph/9807298 (1998).
- [7] E. M. Lifshitz, Zh. Eksp. Teor. Phys. **16**, 587 (1946) [J. Phys. (Moscow) **10**, 116 (1946)].
- [8] I. Jack and L. Parker, Phys. Rev. D **31**, 2439 (1985).
- [9] J. D. Bekenstein and L. Parker, Phys. Rev. D **23**, 2850 (1981).
- [10] J. Schwinger, Phys. Rev. **82**, 664 (1951).
- [11] L. Parker and S. A. Fulling, Phys. Rev. D **9**, 341 (1974).
- [12] B. S. DeWitt, 'The Dynamical Theory of Groups and Fields', in *Relativity, Groups and Topology*, eds. B. S. DeWitt and C. DeWitt (New York: Gordon and Breach); Phys. Rep. **19C**, 297 (1975).
- [13] L. Parker, 'Aspects of Quantum Field Theory in Curved Spacetime: Effective Action and Energy-Momentum Tensor', in *Recent Developments in Gravitation*, eds. S. Deser and M. Levy (New York: Plenum).
- [14] L. Parker and A. Raval, in preparation.
- [15] J. Z. Simon, Phys. Rev. D **43**, 3308 (1991); L. Parker and J. Z. Simon, Phys. Rev. D **47**, 1339 (1993).
- [16] A. A. Starobinsky, Phys. Lett. **91B**, 99 (1980); JETP Lett. **34**, 438 (1981).
- [17] W.-M. Suen, gr-qc/9210018.
- [18] L. Parker, Phys. Rev. Lett. **50**, 1009 (1983).
- [19] L. Parker and A. Raval, Phys. Rev. D **57**, 7327 (1998).
- [20] J. C. Mather *et al.*, Astrophys. J. **420**, 439 (1994).
- [21] E. W. Kolb and M. S. Turner, *The Early Universe* (Addison-Wesley).
- [22] N. D. Birrell and P. C. W. Davies, *Quantum Fields in Curved Space* (Cambridge).
- [23] See, for example, L. Wang, R. R. Caldwell, J. P. Ostriker and P. J. Steinhardt, astro-ph/9901388 and references therein.
- [24] S. Weinberg, *Gravitation and Cosmology: Principles and Applications of the General Theory of Relativity* (John Wiley and Sons, 1972); C. W. Misner, K. S. Thorne and J. A. Wheeler, *Gravitation* (W. H. Freeman and Co., 1973).
- [25] I. S. Gradshteyn and I. M. Ryzhik, *Table of Integrals, Series, and Products* (Academic Press, 1980).

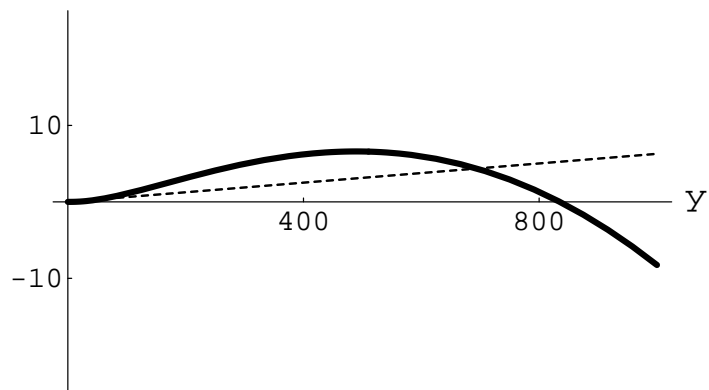


FIG. 1. A plot of the LHS (bold-faced curve) and RHS (dashed line) of Eq. (49), as functions of y , for $\bar{\xi} = 0.033$, $r = 10$ and $\Lambda_o = 0$. The slope of the dashed line increases as r decreases.

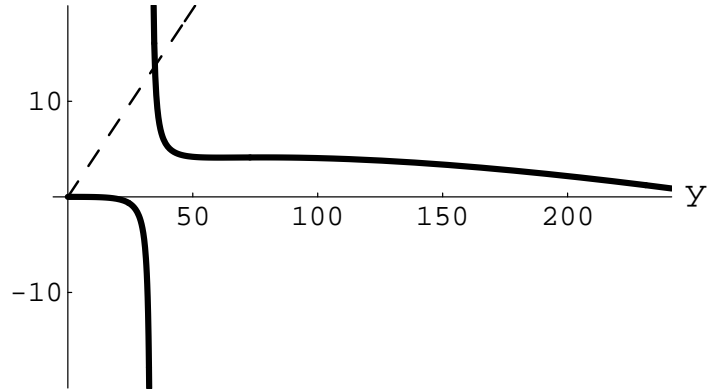


FIG. 2. A plot of the LHS (bold-faced curve) and RHS (dashed line) of Eq. (49), as functions of y , with $\bar{\xi} = -0.03$, $r = 16$ and $\Lambda_o = 0$. As r decreases, the slope of the dashed line increases, and the intersection point is shifted closer to the value $y = -\bar{\xi}^{-1}$. Recall that $r = m^2/m_{Pl}^2$ and $y = R/m^2$.

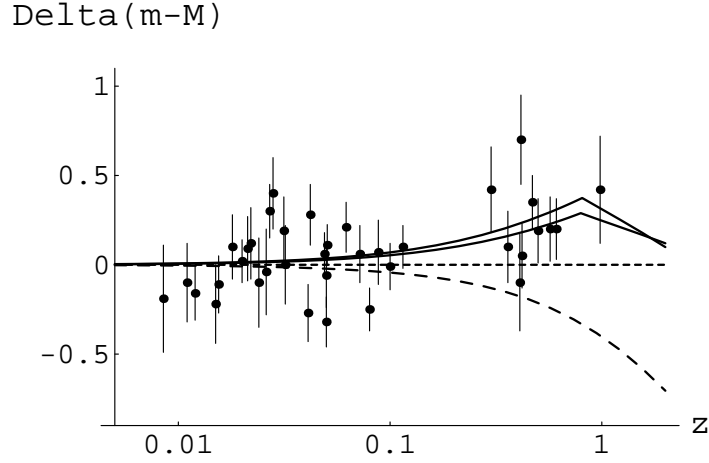


FIG. 3. A plot of the difference between apparent and absolute magnitudes, as functions of redshift z , normalized to an open universe with $\Omega_0 = 0.2$ and zero cosmological constant. The points with vertical error bars represent SNe-Ia data obtained from Ref.[5]. The two solid curves represent the values a) $\bar{m} = 3.7 \times 10^{-33}$ eV and $\Omega_0 = 0.4$ (upper solid curve), and b) $\bar{m} = 3.2 \times 10^{-33}$ eV and $\Omega_0 = 0.3$ (lower solid curve). The horizontal dashed line represents an open universe with $\Omega_0 = 0.2$, and the dashed line curving downward represents a matter-dominated flat universe. Smaller values of Ω_0 also would fit the data (see text after Eq. (112)).

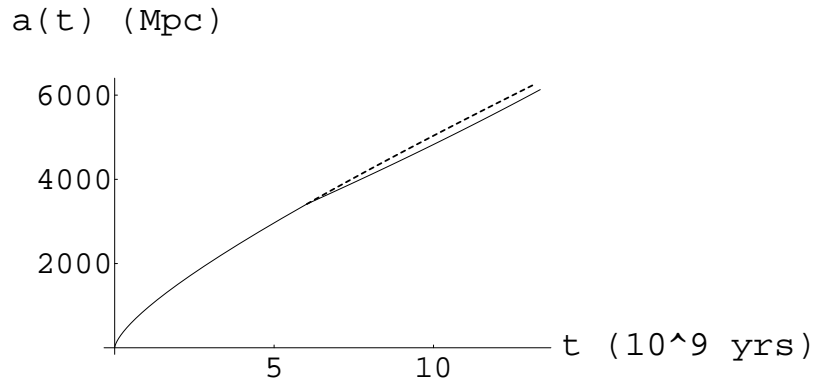
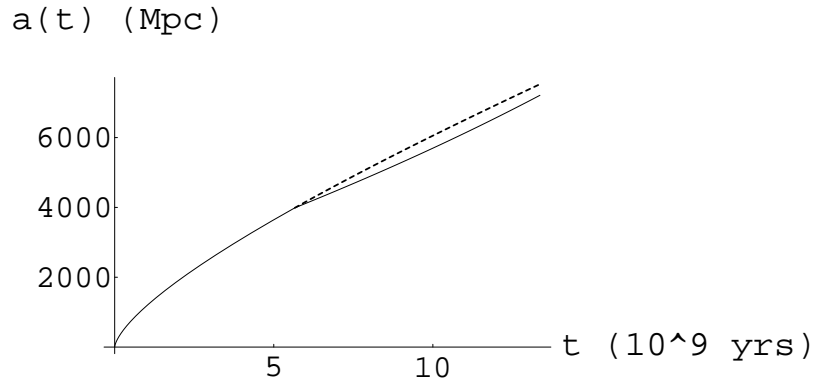


FIG. 4. Two plots of the scale factor versus time for a spatially open model universe in which an initially spatially open matter-dominated cosmology evolves to a de Sitter solution. The parameters for the top model are $\overline{m} = 3.7 \times 10^{-33}$ eV and $\Omega_0 = 0.4$, and for the bottom model, $\overline{m} = 3.2 \times 10^{-33}$ eV and $\Omega_0 = 0.3$. The dashed curves represent a continuation of the open matter-dominated phase.